THE UNIVERSITY of ADELAIDE

Mechanisms of Carbon Sequestration within the Organic Rich Miocene Monterey Formation

Rebecca L. Collett

Geology and Geophysics
School of Earth & Environmental Sciences
The University of Adelaide, Australia

Supervisors: Martin Kennedy and David Chittleborough

Australian Government
Australian Research Council

Table of Contents

Table of Tables

Table of Figures

ABSTRACT

Carbon preservation in the geological past has been an important process for global climate and the onset of glacial events. The majority of carbon preservation occurs in marine continental margin settings that consist of fine grained sediments like the Monterey Formation, California, USA. The mechanisms driving carbon preservation remain highly controversial and the Monterey Formation has served as a prominent test case used to determine these mechanisms. Organic-carbon rich deposits in this formation have been attributed to high organic productivity enhanced fluxes of organic matter (OM) to the sea floor and/or enhanced OM preservation through anoxia. In this study, the Monterey Formation was used as a natural experiment to focus on a new mechanism of carbon preservation, in the form of mineral surface area (MSA) as a control on total organic carbon (TOC). Mineral surface area was determined using the Ethylene Glycol Monoethyl Ether free surface procedure and TOC was derived from high temperature combustion. The relationship between the OM and the surface of the shale samples was viewed using an environmental scanning electron microscope (ESEM) with micron resolution. The major findings indicate a first-order relationship between MSA and TOC, where the mineral surface area adsorption of organic carbon offers an alternative mechanism and control for carbon preservation. This relation is held most strongly in bioturbated intervals as it is indicating oxygenated bottom waters and lower biological productivity intervals which are indicated by carbonate microfossils. Intervals with laminated siliceous sediment reflective of alternative oceanographic hypotheses (linking high productivity and anoxia with organic enrichment) showed lower carbon preservation. Ash beds derived from volcanic glass deposition in the water column showed high surface area from post alteration to bentonite but had low TOC indicating that the association with TOC and MSA occurred in the water column or early diagenetic environment. The MSA within the Monterey Formation is controlled by the abundance of detrital smectitic clays initially formed in hydrologic equilibrium within soils at the prevailing continental climate conditions. Organic matter enrichment in these (marine) continental margin sediments, is thus a function of continental climate. Carbon preservation in the Monterey Formation and similar black shales is not an oceanic mechanism as widely believed, but rather derived through continental controls. An implication of this conclusion is that climate influences detrital clay formation and carbon burial in marine sediments thereby providing a feedback to climate cooling through CO_2 drawdown during high carbon burial events.

KEY WORDS: Monterey Formation, Black Shale, Carbon Preservation, Mineral Surface Area (MSA), Total Organic Carbon (TOC), Smectite.

INTRODUCTION

Carbon preservation in the geological record is a fundamental control of global temperature patterns, oxygen flux to the atmosphere and hydrocarbon source rocks. Carbon burial in sediments is an essential biogeochemical process that acts to regulate global temperature via the drawdown of carbon dioxide while releasing oxygen through photosynthesis (Equation 1). Increases in carbon burial efficiency through time can result in planetary cooling and glaciation (Vincent & Berger 1985), changes in redox conditions in the marine environment (Jenkyns 1980) and widespread deposition of hydrocarbon source rocks (Summerhayes 1981), which have even been attributed to the rise of planetary oxygen leading to metazoan evolution (Kennedy *et al.* 2006).

Equation 1: $light + 6CO_2 + 12H_20 \rightarrow C_6H_{12}O_6 + 6O_2 + 6H_20$

Organic matter (OM) in soils and sediments is widely distributed over the Earth's surface occurring in almost all terrestrial and aquatic environments (Schnitzer 1978). In sediments there are two basic forms of carbon that may be present, (1) inorganic and (2) organic (Schumacher 2002). Naturally occurring organic carbon is derived from reduction of CO_2 by autotrophs and converted back to respiration CO_2 heterotrophic respiration associated with decomposition.

The mechanisms of organic carbon preservation in the geologic record remain controversial with no clear consensus on the dominant mechanism of organic carbon burial emerging. Intervals of globally widespread organic-rich sediment deposition are episodic and imply substantial variations in the carbon cycle, as well as providing targets for hydrocarbon exploration (Ulmishek & Klemme 1990). Research has focused

on better preservation efficiency of reduced carbon in anoxic conditions (Summerhayes 1981), higher organic productivity (Pedersen & Calvert 1990), a greater flux of organic material to sedimentary environments (Pedersen & Calvert 1990) and preservation through rapid burial (Tyson 2001). However, these competing theories have significant ramifications for models of the carbon cycle and the role of the ocean processes regulating it. For example, intervals of high carbon productivity and flux to sediment related to ocean circulation changes have been attributed to the onset of glaciation (Vincent & Berger 1985).

Modern sediments are often used as analogues to study these mechanisms, especially water column process and sediment traps situated on the sea floor. These studies show that only a fraction of organic particles arriving on the seafloor survive early diagenesis (<1m) and have a chance at entering the sedimentary record (Dickens *et al.* 2006). A greater fraction of OM is shown to reach the sea floor in special environments that have been used as analogs to explain geologic enrichments. These include the Oman Margin (Lückge *et al.* 1996) and the Cariaco Basin in Central America (Pedersen & Calvert 1990). However, these special and restricted environments may not be representative of the mechanisms of organic enrichments seen in more continuous open marine settings nor similar to the typical broad intracratonic basin settings associated with most of the black shale typical of specific intervals of the geologic past (e.g. Carboniferous and Miocene). Also, studies of modern carbon burial that include diagenetic reactions in the first 20cm of the sediment indicate that the organic carbon form is different to that found on the sea bed. Essentially, the only carbon that survives transit through the first 20cm of sediment is physically associated

with mineral surfaces and not in a recognizable particulate form (Mayer 1994). For these reasons, sediment trap and water column processes may be unrepresentative of the critical processes influencing geologic enrichment. The exact mechanism of how organic carbon is preserved by minerals remains unspecified, but mineral surface area (MSA) may also be an important, though not commonly considered control in the geologic past (Kennedy *et al.* 2002).

To evaluate the role of MSA, this thesis focuses on the Monterey Formation, California, USA. The Monterey Formation is a classic black shale in the sense that it has high total organic carbon (TOC) content, 6-12 %wt (Isaacs 2001), is regional in its extent and is an economically important hydrocarbon source rock. The Monterey Formation has also been used to explain the onset of northern hemisphere glaciations, a popular hypothesis, evoking climate cooling induced by high productivity and carbon dioxide draw down (Vincent & Berger 1985). The Monterey Formation has been intensively studied as a model system of organic carbon burial, and from these studies no single dominant control is evident (Isaacs 2001). Here, the effects of mineral surface preservation are investigated for the first time to determine if, like in modern sediments, this mechanism played an important role in the past accumulations of organic carbon.

The following research investigates the hypothesis that, in a classic black shale like the Monterey Formation, MSA controls organic carbon preservation. This hypothesis will be tested by comparing measurements of TOC content and MSA on a range of samples from the Monterey Formation and using scanning electron microscopy to identify whether organic carbon exists as discrete particles or has a

mineral association at micron scales. The role of carbon preservation by MSA is poorly known due to the sub-micron scale at which interactions are likely to occur. Thus, the Quanta 450, an environmental scanning electron microscope (ESEM) will be used due to its micron-scale resolution to image and map the distribution of carbon in the Monterey Formation.

A mineral control of organic carbon burial has different implications for carbon burial feedbacks on climate because minerals buried in marine sediments are actually sourced from continental environments. Minerals with high surface area reflect formation under continental hydrologic conditions, but are buried and preserved in continental margin sediments (Hedges & Keil 1995). The Monterey Formation is an example of this. If minerals are responsible for carbon burial, then they could potentially provide a sensitive feedback to changing climate (Kennedy & Wagner 2011). A relation between MSA and TOC in the Monterey Formation would thus have implications for distribution of source rocks that are now attributed to oceanic processes including productivity or preservation. A feedback between climate and carbon burial through detrital mineral surfaces could potentially provide an alternative explanation of climate change at the start of the Cenozoic glaciation.

This paper demonstrates a dominant or first-order influence of MSA on carbon burial that is then modified by other processes in the sediment or water column. This relation has implications for climate change, shale formation, and the distribution of carbon in marine sediments and the implications of other black shale deposits.

This study will test the hypothesis that there is a first-order influence of MSA in carbon burial, following which the organo-mineral complexes are manifested in the

sedimentary column. The implications for climate change, shale formation, the distribution of carbon in marine sediments and other black shale deposits are explored.

GEOLOGICAL SETTING

The Monterey Formation is early to middle Miocene in age and occurs in California, USA, along a present day active margin and consists of fine-grained sediments, which are both source and reservoirs for major quantities of hydrocarbons both on and off-shore California, USA. The Monterey Formation is California's most important source rock and is one of the most important in the United States of America (Bodnar 1990).

One of the most intensively studied sections of the Monterey Formation is the section at Naples Beach, which occurs 25km west of Santa Barbara (Isaacs 2001) and is part of the Santa Barbara basin as seen in Figure 1.

This section of the Monterey Formation is outstanding with regard to its quality of outcrop, continuity and lithological diversity and freshness of weathering. It is regarded as a classic type locality for the Monterey Formation (Hornafius 1994). In many studies the Monterey Formation is considered to be the product of local restricted basin development and the sedimentary processes that govern the present Californian border-land basins (Ingle 1980; Blake 1981; Isaacs 1984; Graham & Williams 1985; Lagoe 1987). However, more recent work reconstructing the margin shows that in the Miocene the depositional environment was a low-gradient slope (Isaacs 2001) and sediments of the Monterey Formation were deposited on an open

margin. The samples collected and used in in this study were taken from the Naples Beach section, on the eastern side of the Dos Pueblos Creek.

The Monterey Formation, is commonly divided into three main facies: lower calcareous facies, a middle transitional facies and a thick upper siliceous facies (Figure 2) (Isaacs *et al.* 1983). The middle facies is predominately phosphatic in composition and the upper facies is composed of diatomaceous rocks and their diagenetic equivalents (Isaacs *et al.* 1983). The widespread siliceous facies has been interpreted to record rapidly deposited diatom ooze, indicating high plankton productivity and is attributed to intensified upwelling in the late Miocene (Isaacs *et al.* 1983).

The ages of the formation range from 9.4-14.3 Ma with the TOC content of the shales varying from 6-12.6 wt% (Follmi *et al.* 2005). As seen in Figure 2, the lower calcareous facies is between 18.4-13.6 million years old, whereas the upper siliceous facies is as young as 6.7 million years old.

The Monterey Formation overlies the lower Miocene Rincon Formation, which consists of clayey mudstones containing dolomite concretions and siltstone (Hornafius 1994;Follmi *et al.* 2005). The Rincon Formation is capped by a thin layer of bentonite as seen in Figure 2, which is the diagenetic product of a siliceous ash and defines the contact between the Rincon Formation and the Monterey Formation. The Sisquoc Formation is upper Miocene and lower Pliocene in age (Ingle 1981; Barron 1985). The contact to the overlying Sisquoc Formation is marked by an erosive surface and transition from diatomite to clayey siliceous mudstones (Follmi *et al.* 2005).

The mineralogical composition of the Monterey Formation at Naples Beach is influenced by early digenetic processes that have especially led to the precipitation of

phosphate, which was formed at a very early stage of digenesis (Follmi *et al.* 2005). Diagenesis of the Monterey Formation typically involved the widely recognized sequence of silica phases, from an initial biogenic opal-A to diagenetic quartz (Isaacs *et al.* 1983). Accompanying this sequence was a typical diagenetic succession of rocks: diatomites and diatomaceous shales to opal-CT cherts, porcelanites, and mudrocks to quartz cherts, porcelanites, and mudrocks (Isaacs *et al.* 1983). Diagenesis of carbonate sediments in the Monterey Formation consists of six major processes: cementation, microbial micritization, neomorphism, dissolution, compaction and dolomitization. Thermal generation of hydrocarbons within more deeply buried portions of the Monterey Formation has resulted in migration and oil staining, and bitumen accumulation along fractures within the formation (Figure 3).

The Monterey Formation is an older Miocene stratigraphic unit. It shows different patterns of thickness variation and facies arrangements that are not directly related to present structural or topographic basin configurations. Subsidence and volcanism indicated in this formation is a manifestation of early Miocene regional crustal extension (Tennyson & Isaacs 2001). Through most of the ensuing Miocene (10 million years) a blanket of siliceous, phosphatic and/or calcareous, clastic-poor, organic matter rich mudrock accumulated, burying the old fault-controlled topography (Tennyson & Isaacs 2001). By the late Miocene (6 Ma) the region began to experience compressive deformation that intensified into the Pliocene (Tennyson & Isaacs 2001). Folds and reverse faults widespread throughout the area indicate that compressive deformation within the Monterey Formation was significant (Tennyson & Isaacs 2001).

ANALYTICAL METHODS

The samples were collected by hand from clean coastal outcrops tied to Follmi's section (2005) within the different evident facies of the middle Monterey Formation. They were then air-dried, ground and passed through a 2.0mm (10 miesh) sieve. Analytical work carried out on the samples involved measurement of MSA using the Ethylene Glycol Monoethyl Ether (EGME) free surface procedure. These samples then underwent inorganic carbonate and organic carbon analysis by high temperature combustion, as well as carbonate carbon analysis through the use of a manometer to determine TOC.

Organic Matter removal

Analytical techniques for the removal of OM from samples follow those of Schumacher (2002) and Jackson (1979). A fraction of the shale samples obtained from the Naples Beach section of the Monterey Formation underwent OM removal through the hydrogen peroxide digestion method (Mayer, 1994). The hydrogen peroxide digestion method destroys the organic matter by oxidation. The method involves the addition of concentrated hydrogen peroxide (30 wt %) to a sediment, where it is continually added to the sample until frothing of the sample ceases, a sign that the reaction is complete. Once the digestion process is completed the sample is dried at 105°C for a period of 24 hours.

The peroxide digestion method has several limitations in that it is only semi-quantitative (Schumacher 2002) and the oxidation of OM is often incomplete (Robinson 1927). This was not a significant problem in this study because removal of

OM was performed only to check for any effects on measured surface area and to determine if OM itself had a measureable surface area.

Calcium exchange

Analytical techniques for the exchange of calcium on the cation exchange sites follow those of Moore & Reynolds (1989). All samples from the Monterey Formation underwent this process so that a known ion was on the exchange sites of the clays. The samples were weighed (3g) and placed into a centrifuge tube, where 10-20ml of 1M calcium chloride was added to the sample. The sample and added calcium chloride was then shaken for five minutes to allow for the interaction of the entire sample with the calcium chloride solution. The samples were then left for 24 hours to allow for the sediment to settle out of suspension. The supernatant was then siphoned off.

The samples then underwent the same procedure but with deionised water, to remove any excess calcium that was leftover on the sample's exchange sites. This procedure was repeated twice, with both processes allowing 24 hours for the suspension to settle out of solution, and the supernatant was siphoned off. The samples then underwent the same procedure as with the calcium chloride but with ethanol, where there was only one repeat.

If the ethanol suspensions remained after 24 hours, the samples were centrifuged for 3 minutes at 2400 reps. The samples were then oven dried at 105°C for 24 hours.

Ethylene Glycol Monoethyl Ether analysis

Analytical techniques for EGME analysis to obtain MSAs follow those of Eltantawy & Arnold (1973), Churchman *et al.* (1991) and Tiller & Smith (1990), where the "Free Surface" procedure was used. Ethylene Glycol Monoethyl Ether (3ml) was added to 1g

of oven dried sediment in a glass vial and a slurry was formed. The empty glass vial and cap was initially weighed, and then weighed again with the ground shale sample to allow for the calculations of MSA. A diamond tip pen was used to label the sample due to the strength of the EGME.

The slurry was then allowed to stand for 30 minutes in a sealed vacuum chamber, containing 200g of dried calcium chloride and 40ml of EGME in separate containers. The vacuum was then evacuated for 30-60 minutes and the samples were stood under vacuum until the end point was reached. This occurred when the samples were dry and still in equilibrium with the free surface of EGME in the chamber whilst maintaining a constant mass. This took 5-7 days as some samples dried out quicker than others depending on the mineralogy of the sediment sample. When dry air was emitted into the chamber, it was important to immediately seal the glass weigh bottles with their lids to decrease the amount of water to compete with the EGME and to attach to the clay surfaces within the samples. The MSA was calculated from the mass of the retained EGME liquid under the assumption that a monomolecular layer was adsorbed on the surface.

It was important to maintain a free surface of EGME as it tended to evaporate after a couple of days. Also it was important to turn over the calcium chloride as the efficiency of it as a sink for the EGME evaporated from the sediment slurry was relatively quick and a hard impenetrable surface to the EGME formed. The analysis from the MSA methods were used to determine the surface area present on the clays.

Total carbon, inorganic carbon and organic carbon

Analytical techniques for TOC analysis followed those of Soil Chemical Methods Australia (Rayment & Lyons 2010), where the total carbon, which includes inorganic carbonate and organic carbon analysis, was carried out at the University of Maine (USA) by high temperature combustion using a Perkin-Elmer 2400B Elemental Analyser. This procedure involved ignition of the sediments at high temperature in a stream of oxygen followed by detection of CO_2 liberated by an infrared detector.

The inorganic carbon (carbonate) analysis was undertaken at the University of Adelaide (Australia) using a manometer, where 1g of a sample was added to 20ml of 4M hydrochloric acid in a sealed vessel. The change in volume associated with the conversion of carbonate carbon to CO_2 was used to define the amount of inorganic carbon present in the samples after calibration with a pure carbonate standard.

TOC was determined by difference, i.e.

Total Carbon =Inorganic Carbon + Organic Carbon

Every tenth sample was duplicated, and one sample underwent the procedure ten times to determine the error in the experiment.

Environmental Scanning Electron Microscope Imaging and Mapping

The Quanta-450 environmental electron microscope was used to take images of the shale samples at the micron-scale, to map carbon over the surface of the samples and to use point analysis to determine where the carbon occurred.

Four samples were chosen to provide a range in TOC values. Rock chips for each of these samples were mounted and carbon coated to minimise scatter. The TOC values ranged from 4-21%.

The Quanta-450 ESEM was used in the high vacuum mode with a spot size of 5.5 and a beam voltage of 20kv to allow for higher counts for carbon mapping. Both secondary electron and back scatter detectors were used to obtain images, and a SDD X-ray defector was used for the carbon mapping/point analysis. The secondary electron images showed the topography of the samples due to secondary electrons being low energy electrons (<50eV). Therefore, only the secondary electrons from first few atomic layers escape. Topographic highs appear as bright spots and areas of topographic lows appear as dark regions (Wade 2010), whereas the back scatter images showed the contrasts due to atomic numbers. This is because backscattered electrons are high energy electrons scattered from atoms (up to 50nm) below the surface of the sample, where information is obtained from the Z contrast of the sample (Z = atomic number) (Wade 2010). Regions containing atoms with high Z values are viewed as bright regions, whereas dark regions are areas with atoms that have low Z values (Wade, 2010).

RESULTS

Mineral Surface Area vs. Total Organic Carbon

Comparison of TOC with MSA (Figure 4a-b) shows a first-order linear relationship (R^2=0.53 and 0.85) across a range of TOC (non-carbonate diluted intervals) from 1-27% validating the hypothesis. The study covered three lithofacies, which show a similar loading ratio of OM to MSA. There is a first-order relationship (primary relationship) and a second-order relationship present in the following data. The first-order

relationship is the primary control and occurs as a linear function of MSA, whereas the second relationship results in divergence of data to the right of the linear array.

The samples were taken from different stratigraphic intervals. Samples from from the base to 900 metres can be viewed in Figure 4a. Figure 4b shows samples in the stratigraphic interval of 900-1150 metres, and Figure 4c shows samples in the stratigraphic interval of 1150-1600 metres. The lower facies of the Monterey Formation consists of phosphatic- and mudstone-rich sediments, where dolomite and clay/shale lithologies are also present. The middle facies of the formation consist of phosphatic- and porcelanite-rich lithologies and the upper facies of the formation is composed of porcelanite lithologies.

The X axis (Figures 4, 5, 6, 7) is the MSA of the samples minus the carbonate percent, which has been subtracted in order to remove the effects of dilution by carbonate causing an auto correlation with TOC. The Y axis (Figures 4, 5, 6, 7) is the TOC minus the carbonate percentage. The MSA and the TOC have been normalised to the siliciclastic fraction so that the overall result would not be affected and driven by the carbonate variation (2-50%).

Mineral surface area is the combined surface area of the external and interlayer sites of the minerals in the sediment samples. It was measured using the EGME method, thereby providing a total surface area determination of the smectite clays versus external only typically reported from Brunauer–Emmett–Teller instrument (BET) measurements and determined by N_2 adsorption. This allows for the interlayer loading of OM onto the surface areas of the minerals assuming that interlayer sites are accessible to organic compounds. Smectite has a surface area that is an order of

magnitude greater than illite because EGME can enter the interlayer sites in smectite but not illite. Interlayer preservation can thus, lead to significant carbon preservation with TOC as high as 25% for a single molecular monolayer (Kennedy and Wagner 2011).

The distribution of the data relative to a monolayer equivalent line (Mayer 1994) provides some insight into the carbon and MSA association. As seen in Figure 5 the laminated mudstone lithology is dominant in the Monterey Formation and has a positive relationship with R^2=0.66. Different extents of loading of organic matter onto the surface area of the minerals account for the difference in the slope.

The following seven lithologies were distinguished in the Monterey Formation (Table 1). A comparison of TOC and MSA in the different lithologies shows a first order linear relationship for carbonate cements (Figures 5 and 6) R^2= 0.82, phosphatic mudstone (Figure 7) R^2= 0.79 and clay shale (Figures 5 and 7) R^2= 0.97. The nodular mudstone had a positive relationship, R^2= 0.59 (Figure 7), although there was scatter in the data. The porcelenite and ash lithologies showed no relationship between MSA and TOC (Figures 6 and 7).

Mineral Surface Area

Samples of the Monterey Formation were analysed after OM was removed so that the surface area of the bare mineral surfaces in a sample could be measured. This would determine whether adsorption of the EGME on the OM was an important contributor to the total MSA and to determine whether EGME was measuring OM surface area, and thus, scaling with TOC. The samples with OM removal were plotted against samples that still had OM present (Figure 8). Removal of the OM tended to

cause variable effects on the MSA. Across the majority of the samples a tendency existed for the sediments to give higher surface area in the presence of OM. In two cases, OM removal led to a significant increase in surface area, which could be explained by either the creation of high surface area oxy-hydroxide phases or Fe-oxides or by the removal of OM occluding microporosity and interlayer space of 2:1 clays. This occurrence has been recorded before in Weiler and Mills (1965) and Titley (1987), where the relationship could also be attributed to the exposure of small pores, which was originally blocked by the OM. Mayer (1994) concluded that the occurrence of the MSA decreasing could be attributed to dissolution of roughness elements on the mineral, which are responsible for surface area. Overall, Mayer (1994) and Kennedy & Wagner (2011) have shown that there is no significant difference in surface area indicating that OM does not interact with EGME. Therefore, in this experiment excessive hydrogen peroxide digestion may have occurred with a number of samples destroying the MSAs.

Error Analysis

The MSA mean of the Clay Mineral Society SAz Smectite was 805.25 m^2g^{-1} with a standard error of ± 3.63 and the Clay Mineral Society Mancos had a mean MSA of 210.06 m^2g^{-1} with a standard error of ± 0.64. Overall, the average percentage coefficient of variation between the standards was 1.23, which was acceptable. Therefore. it can be assumed that all of the Monterey Formation samples analysed had a percentage coefficient variation of 1.23 for the MSA. The TOC mean of the Clay Mineral Society SAz Smectite was 0.02% with a standard error of ± 0.0007 and the Clay Mineral Society Mancos had a mean TOC of 2.47 % with a standard error of ± 0.27.

Overall, the average percentage coefficient of variation between the standards was 7.20, which was satisfactory.

Environmental Scanning Electron Microscope Imaging

The ESEM was used to determine where the organic carbon was located, how it was occurring and if there were any mineral or structural relationships, such as preservation of organic particles in mineral pores. Evidence of samples that showed greater carbon than the monolayer equivalent loading imply that addition of particulate material) only occurred in one sample (Figure 4a). Particulate carbon was not evident in ESEM images. However, to image the distribution of carbon a greater than µm scale of resolution was necessary. Diatoms and other broken up fossil matter was also imaged. Figure 9 shows an image of a diatom using the secondary electron detector (a), a secondary image of the outer surface of a diatom (b), a carbon map of the same diatom (c), and, a point analysis of the outer edge of the diatom (d). The carbon map shows that carbon is present on the surface and it concentrates around the surface of the diatom where the clay platelets (Figure 9b) are present inferring the carbon is clay, and not diatom associated.

DISCUSSION

Black shales occur episodically throughout the geological record and signify high organic carbon enrichment relative to background sediments. Black Shales are most common in greenhouse periods (Negri *et al.* 2008) and are assumed to correspond with sluggish oceanographic circulation patterns resulting in low dissolved oxygen, such as in the Late Cretaceous. However, the Monterey Formation contrasts with

these examples as it is an organic carbon enrichment in an ice-house period. Organic carbon enrichment in the Monterey Formation has been hypothesized to reflect enhanced upwelling as a function of the California current and nutrient delivery to ecosystems driving heightened biological productivity and sedimentation of OM to the sea floor (Vincent & Berger 1985). This enhanced carbon burial is linked to a positive feedback driving global cooling and the onset of northern hemisphere glaciation in the Monterey Formation Hypothesis (Vincent & Berger 1985). The Monterey Formation was used in this study as a natural experiment of how organic carbon enters the geological record.

Determination of the origin of organic carbon in sediments is difficult, as its composition is not readily visible to the naked eye or with the use of a light microscope. Organic carbon however, can be visible with the use of an electron microscope. There were no visible discrete concentrated areas of organic carbon identified where the organic compound could be imaged (Figure 9). Alternatively, the organic matter could be at submicron scales in these samples that they may only be visible using a much higher magnification. As determined by Mayer (1994) and Hedges & Keil (1995), the bulk of organic compounds cannot be physically separated from the mineral phase in sediments below 20cm of the sea floor. Above the 20cm, particulate material is more common. This suggests that the occurrence of organic carbon could be attributed to mineral associations. Currently, the association between MSA and TOC is established in modern sediments, and is less established in ancient marine sediments.

The relationship and occurrence of organic carbon had to be tested indirectly through the use of bulk properties because it was not imageable with the ESEM. The TOC was tested as a function of MSA to test the hypothesis that there is a strong influence of mineral preservation effects in ancient sediments as well. A linear relationship is present in some facies of the Monterey Formation (Figure 4).

The majority of clay minerals are formed in soils and are transported to continental margins settings. Pedogenic clays thus reflect continental climates, not marine processes. The presence and abundance of clay minerals in marine sediments is dependent upon specific climate conditions as well as provenance with volcanic sediments prone to smectite composition. Thus they form a link between continental climate variations as a function of clay mineralogy with marine carbon burial (Kennedy & Wagner 2011). As a result enhanced MSA could be a feedback to climatic changes (Figure 10). Clay mineral changes may be significant to climate because marine sediments, like the Monterey Formation, are made up of 60% mudstone (Blatt *et al.* 1980), which consists of greater than 60% clay. Figure 10 shows a feedback system, where carbon burial increases with warming through MSA control on carbon burial, driving the temperature down through atmospheric carbon dioxide sequestration in organic carbon preserved on clay minerals. This then forces the climate to become colder, reducing MSA through clay composition changes thus reducing organic matter sequestration and carbon dioxide removal from atmosphere. This outlines a possible feedback between continental weathering, clay formation and erosion and carbon burial (Kennedy & Wagner 2011).

The MSA values found in this study are 140-450 m^2g^{-1} which are high relative to quartz (<10 m^2g^{-1}), kaolinite (20 m^2g^{-1}) and illite (<90 m^2g^{-1}) (Kennedy & Wagner 2011). The reason these values are large is because of the high smectite content (which was determined with the Clay Mineral Society SAz Smectite surface area to be 805.25 m^2g^{-1}. Imogolite, allophane, and iron oxides also all have high surface area but are geologically unstable and are unlikely to be present in these sediments (Theng *et al.* 1982). Conversely, OM has comparative surface areas in soils but little surface area in mature sediments when functional groups are lost (Kennedy & Wagner 2011). There is no loss of surface area with removal or organic matter (figure 8). Therefore, the high MSA in the Monterey Formation is a function of smectite deposition.

The TOC values are variable between lithologies in the Monterey Formation (Figure 5). A lot of TOC means a lot of surface area which is only possible if interlayers are active and only smectite has accessible/hydratable interlayers. This study infers that the high TOC values of the Monterey Formation (<26%) is related to the activity of internal surfaces of the mineral where organic carbon preservation occurs according to the bulk property constraints provided by the TOC-MSA relation in Figures 5, 6, and 7.

There are other influences likely affecting the TOC-MSA relation based on the variability of slope and of values evident in Figure 5. Different mechanisms of carbon deposition occurred due to the distribution between the lithologies. A sequence of samples fall off the monolayer equivalent line, which are indicative of a series of processes involved in organic carbon loss (Figure 11). The organic carbon loss (Figure 11-B) can be attributed to thermogenic degradation or microbial respiration. However, several data points are displaced from the line towards a lower TOC, where the MSA-

TOC relation may not be valid due to lithological controls, i.e. an ash bed. A sequence of samples (Figure 11-A) fall above the line and are attributed to organic carbon addition. Organic carbon addition could possibly be due to particulate carbon, migrated hydrocarbons or multilayer loading. Multilayer loading cannot be confirmed with the data collected, as there are only a few isolated samples, but the organic carbon addition is consistent with particulate carbon. Nevertheless, the culmination of these observations supports MSA as an organic carbon burial mechanism for majority of the lithologies present in the Monterey Formation.

A range of lithologies from the Monterey Formation show that the MSA-TOC relation accounts for organic carbon burial in marine sediments. As seen in Figures 6 and 7, the laminated mudstone, carbonate cement, nodular mudstone, phosphatic mudstone and clay shale lithologies all show an effect of MSA on TOC content. The claystone lithology has the strongest relationship (R^2=0.97) and is associated with lower biologic productivity in the water column which is evidence against the leading model of organic carbon enrichment. The Monterey Formation has been replaced selectively by dolomite and subsequently fractured, brecciated, and relithified with several generations of dolomite cement (Roehl 1981). The carbonate cement lithology also shows a relationship and is further evidence for internal organic cycling in upper sediments, where they are a product of sulphate oxidation of carbon in sediments. Phosphatic intervals in the Monterey Formation are dominant and show areas where significant organic diagenesis occurred, which resulted in OM oxidation (Follmi *et al.* 2005). Phosphate traces the amount of organic carbon loss from OM (Follmi *et al.*

2005) as wherever OM is oxidised, phosphorous remains. However, the MSA-TOC relationship is not consistent in all lithologies that occur in the Monterey Formation.

The ash and porcelanite lithologies do not show a relationship between MSA and TOC (Figures 6 and 7). This is consistent with the hypothesis in the case of ash as it is not associated with OM when deposited due to the clay composition of an ash being a post-depositional product of volcanic loss. This is indicative of how proficient organic carbon preservation is in a depositional environment. The porcelanite lithology is interesting as it has significant surface areas and deposition occurred in marine waters that were likely anoxic (laminated and bioturbaceous), where almost no OM was preserved. This implies that specific clay minerals may have properties of carbon preservation that generic surface area does not provide. This is likely a function of charge, as well as the interlayer of smectite clays.

Mineral surface area provides a control on organic carbon preservation in marine sediments, since MSA is a function of continental processes. Thus organic carbon preservation is not only oceanically controlled as according to the dominant paradigm. This data argues against the Monterey Formation hypothesis (Vincent & Berger 1985), which predicts higher oceanic circulation rates leading to organic carbon control.

The data from the Monterey Formation was plotted with additional data from other black shale units (Kennedy & Wagner 2011) (Figure 12c). These data were normalised to a similar suite of standards, thereby establishing a valid comparison with the Monterey Formation. As observed in Figure 12c, the Cretaceous examples from the Ivorian Basin, West Africa, and the samples from the Monterey Formation show similar grouping. The Monterey Formation samples have similar slope and proximity on the

cross-plot with the Ivorian Basin bioturbated and laminated interval data (Figure 12c). Therefore it can be inferred that the preservation of organic carbon in the Monterey Formation and the depositional environment in the Ivorian Basin, West Africa, could be similar. However, this can only be speculated as the similar redox evidence was not collected in samples of the Monterey Formation.

There are different loadings of organic carbon onto the surface area of the smectite mineral. Figure 13 shows that there are four different models for surface loading (Figure 13); A, B, C and D, which can occur. This is shown by the slope of the relationship between the MSA and the TOC content. Models A and B show organic carbon addition, where A is limited by surface area and is saturated by OM, and B has the same slope as the monolayer equivalent line but has greater number of interlayer sites for loading. Models C and D show organic carbon loss, where C has lost a proportionality of organic carbon through the oxidation of the external edges of the loading sites. However, the organic carbon in C is still proportional to the MSA. Model D is organic carbon limited, where the loading rate is smaller than the other models; leading to excess surface area.

Particulate OM is able to reach the sea floor passively (sedimentation), and actively (organism filter feeder) (Zonneveld *et al.* 2009). As previously discussed one sample in the Monterey Formation shows evidence of particulate OM (Fig 12c, red circle). However, particulate OM is not evident on the SEM images (Fig 12d). Mayer (1994) found that particulate OM only survives to a depth of 20cm below the seafloor (Fig 12b). High fluxes of OM in part form from super-productive episodes as hypothesised in the Monterey Formation but did not enter the geologic record. This is suggested in

the Monterey Formation by the abundance of phosphate nodules, which are suggested to record respiration of significant OM, leaving phosphate behind as stated previously (Fig 12a). This supports the idea that mineral surfaces provide preservative effects that can transfer terrestrially derived organic carbon to the sediment reservoir and that the oceanographic processes, such as productivity and anoxia, are restricted to shorter internal cycles between the upper sediments and the water column.

CONCLUSION

The major findings in this study validate the hypothesis that; MSA enhances organic carbon preservation and provides a first-order control of carbon burial in marine sediments. The relationship between MSA and TOC, however, was not consistent for the variety of lithologies occurring in the studied section, indicating that there are conditions that modify the relationship. For example, while volcanic ash beds have high mineral surface area, that surface area was established after deposition and shows no relation with TOC. At the micron scale, the OM could not be resolved using ESEM implying that discrete organic particles were not present in the samples studied and that the OM (comprising upto 20% of the weight of the sample) was at the micrometer scale. It implies that this OM existed as organo-mineral complexes with carbon on surfaces likely occurring at micrometer scales. Comparison of TOC with MSA from different intervals of the Monterey Formation show the surprising result that high TOC intervals do not correlate with the high productivity anoxic interval of the formation, but rather within the bioturbated (oxygenated) low productivity clay-rich intervals. This is evidence against the dominant paradigm for carbon enrichment in the

Monterey Formation of anoxia and high productivity, reinforces the first-order controls of MSA. Surface area of minerals is created in continental soils under particular climatic conditions. Thus, implying that the mineral properties of the sediments in marine sediments are sometimes at least a function of continental climate. Changes in climate then can feedback on carbon burial, which is an important control on climate through atmospheric CO2 drawdown and reduced greenhouse warming.

There are some micro/nano techniques that could help resolve the nature of organo-mineral associations in future research. The chemistry, form and distribution of the OM may be resolved by high resolution transmission electron microscopy (TEM) and synchrotron based small angle X-ray scattering combined with nano secondary ion mass spectrometry. Further research could also resolve whether the TOC-MSA relationship can change on a timescale relevant to future climate.

ACKNOWLEDGMENTS

This work was funded by the Australian Research Council. I would like to acknowledge my amazing supervisor Martin Kennedy for all of his support, enthusiasm, motivation and inspiration throughout the year. I would also like to thank David Chittleborough, my secondary supervisor for his advice and mentoring.

Jock Churchman and Jeffrey Baldock who are affiliates with the University of Adelaide are kindly thanked for their assistance and guidance. Acknowledgments are also given to Lawrence Mayer from the University of Maine for guidance and analytical TOC work carried out on the samples. Ken Neubauer and Ben Wade from Adelaide Microscopy are thanked for their assistance on the Quanta 450, and John Stanley for assistance with anything needed in the Mawson laboratory.

I would also like to thank Katie Howard for providing so much assistance and support and Rob Klaebe for being my partner in crime for honours. I would also like to thank the Geology and Geophysics Honours year of 2011. I would like to thank my family, especially my parents for their encouragement and support as well as the Baldocks who have helped me become a scientist. Lastly I would like to thank Joshua for believing in me.

REFERENCES

BARRON J. 1985. *Miocene to Holocene planktic diatoms in Plankton stratigraphy*. Cambridge University Press, Cambridge.

BLAKE G. 1981. Biostratigraphic relationship of Neogene benthic foraminifera from the southern California outer continental bordeland to the Monterey Formation. *In:* Garrison R. & Douglas R. eds., *The Monterey Formation and Related Siliceous Rocks of California*, pp 1-14, Pacific Section SEPM, Los Angeles.

BLATT H., MIDDLETON G. & MURRAY R. 1980. *Origin of Sedimentary Rocks*. Prentice Hall, New Jersey.

BODNAR R. 1990. Petroleum migration in the Miocene Monterey Formation, Califronia, USA: constraints from fluid-inclusion studies. *Mineralogical Magazine* **54**, 295-304.

CHURCHMAN G. J., BURKE C. M. & PARFITT R. L. 1991. Comparison of various methods for the determination of specific surfaces of subsoils. *Journal of Soil Science* **42**, 449-461.

DEPAOLO D. & FINGER K. 1991. High-resolution strontium-isotope stratigraphy and biostratigraphy of the Miocene Monterey Formation, central California. *Geological Society of America Bulletin* **103**, 112-124.

DICKENS A., BALDOCK J., SMERNIK R., WAKEHAM S., ARNARSON T., GÉLINAS Y. & HEDGES H. 2006. Solid-state 13C NMR analysis of size and density fractions of marine sediments: Insight into organic carbon sources and preservation mechanisms. *Geochimica et Cosmochimica Acta*, 666-686.

ELTANTAWY I. & ARNOLD P. 1973. Reappraisal of ethylene glycol monoethyl ether (EGME) method for surface area estimations of clays. *Journal of Soil Science* **24**, 232-238.

FOLLMI K., KAENEL E., STILLE P., JOHN C., ADATTE T. & STEINMAN P. 2005. Phosphogenesis and organic-carbon preservation in the Miocene Monterey Formation at Naples Beach, California-The Monterey hypothesis revisited. *Geological Society of America Bulletin* **117**, 589-619.

GRAHAM S. & WILLIAMS L. 1985. Tectonic, depositional, and diagenetic history of Monterey Formation (Miocene), central San Joaquin basin, California. *America Association Petroleum Geology Bulletin* **69**, 385-411.

HEDGES J. I. & KEIL R. G. 1995. Sedimentary organic matter preservation-an assessment and speculative synthesis. *Marine Chemistry* **49**, 137-139.

HORNAFIUS J. E. 1994. *Field Guide to the Monterey Formation between Santa Barbara and Gaviota, California*. American Association of Petroleum Geologists, Pacific Section, California.

INGLE J. 1980. Cenozoic paleobathymetry and depositional history of selected sequences within the southern California continental borderland. *In*, *Studies in Micropaleontology*, pp 163-195, Cushman Foundation, Washington.

INGLE J. 1981. *Origin of Neogene diatomites around the North Pacific rim in Monterey Formation and related siliceous rocks of California*. Society of Economic Paleontologists and Mineralogists, Pacific Section.

ISAACS C. 1984. Hemipelagic deposits in a Miocene basin, California: Toward a model of lithologies variation and sequence. *In:* Stow D. & Piper D. eds., *Fine-Grained Sediments: Deep-Water Processes and Facies*, pp 481-496, Blackwell, Oxford.

ISAACS C. 2001. Depositional framework of the Monetery Formation, California. *In:* Isaacs C. & RullKotter J. eds., *The Monterey Formation: from Rocks to Molecules*, pp 31-59, Columbia University Press, New York.

ISAACS C., PISCIOTTO K. & GARRISON R. 1983. Chapter 15 Facies and Diagenesis of the Miocene Monterey Formation, Califronia: A Summary. *Developments in Sedimentology* **36**, 247-282.

JACKSON M. 1979. *Soil Chemical Analysis* ((2nd ed.) edition). (Advanced Course).

JENKYNS H. C. 1980. Cretaceous oceanic anoxic events from continents to oceans. *Journal of the Geological Society of London* **137**, 171-188.

JENNY H. 1941. *Factors of Soil Formation*. McGraw-Hill, New York.

KENNEDY M. & DERKOWSKI A. 2007. Organic enrichment controlled by smectite clay minerals in the Miocene Monterey Formation and Cretaceous Pierre Shale. *Geophysical Research Abstracts* **9**.

KENNEDY M., DROSER M., MAYER L. M., PEVEAR D. & MROFKA D. 2006. Late Precambrian oxygenation; Inception of the clay mineral factory. *Science* **311**, 1446-1449.

KENNEDY M. J., PEVEAR D. R. & HILL R. J. 2002. Mineral surface control of organic carbon in black shale. *Science* **295**, 657-660.

KENNEDY M. J. & WAGNER T. 2011. Clay mineral continental amplifier for marine carbon sequestration in a greenhouse ocean. *Proceedings of the National Academy of Sciences of the United States of America* **108**, 9776-9781.

LAGOE M. 1987. Middle Cenozoic basin development, Cuyama basin, California. *In:* Ingersoll R. & Ernst W. eds., *Cenozoic Basin Development of Coastal California*, pp 173-206, Prentice-Hall, New Jersey.

LÜCKGE A., BOUSSAFIR M., LALLIER-VERGÈS E. & LITTLE R. 1996. Comparative study of organic matter preservation in immature sediments along the continental margins of Peru and Oman. Part I: Results of petrographical and bulk geochemical data. *Organic Geochemistry* **24**, 437-451.

MAYER L. M. 1994. Surface area control of organic carbon accumulation in continental shelf sediments. *Geochimica et Cosmochimica Acta* **58**, 1271-1284.

MOORE D. & REYNOLDS R. 1989. *X-Ray diffraction and the identification and analysis of clay minerals*. Oxford University Press, Oxford.

NEGRI A., FERRETTI A., WAGNER T. & MEYERS P. A. 2008. Phanerozoic organic-carbon-rich marine sediments: Overview and future research challenges. *Palaeogeography, Palaeoclimatology, Palaeoecology* **273**, 218-227.

PEDERSEN T. F. & CALVERT S. E. 1990. Anoxia vs Productivity-what controls the formation of organic carbon rich sediments and sedimentary rocks. *Aapg Bulletin-American Association of Petroleum Geologists* **74**, 454-466.

RAYMENT G. & LYONS D. 2010. *Soil Chemical Methods-Australasia* (Australian Soil and Land Survey Handbooks Series). CSIRO Publishing, Collingwood.

ROBINSON W. 1927. The determination for organic matter in soils by means of hydrogen peroxide. *Journal of Agricultural Research* **34**, 339-356.

ROEHL P. 1981. Dilation brecciation: proposed mechanism of fracturing, petroleum expulsion, and dolomitization in Monterey formation, California. *America Association Petroleum Geology Bulletin*, 980-981.

SCHNITZER M. 1978. *Humic substances: Chemistry and reactions* (Soil Organic Matter). Elsevier Scientific Publishing Co., New York.

SCHUMACHER B. 2002. Methods for the determination of total organic carbon (TOC) in soils and sediments. *United States Environmental Protection Agency*.

SUMMERHAYES C. P. 1981. Organic facies of Middle Cretaceous black shales in deep North Atlantic. *AAPG Bulletin* **65**, 2364-2380.

TENNYSON M. & ISAACS C. 2001. Geologic Setting and Petroleum Geology of Santa Maria and Santa Barbara Basins, Coastal California. *In:* Issacs C. & Rullkotter J. eds., *The Monterey Formation from Rocks to Molecules*, Columbia University Press, West Sussex.

THENG B., RUSSELL M., CHURCHMAN G. & PARFITT R. 1982. Surface Properties of Allophane, Halloysite and Imogolite. *Clays and Clay Minerals* **30**, 143-149.

TILLER K. G. & SMITH L. H. 1990. Limitations of EGME retention to estimate the surface area of soils. *Australian Journal of Soil Research* **28**, 1-26.

TITLEY J., GLEGG G., GLASSON D. & MILLWARD G. 1987. Surface areas and porosities of particulate matter in turbid estuaries. *Continental Shelf Research* **7**, 1363–1366.

TYSON R. V. 2001. Sedimentation rate, dilution, preservation and total organic carbon: some results of a modelling study. *Organic Geochemistry* **32**, 333-339.

ULMISHEK G. & KLEMME H. 1990. Depositional controls, distribution and effectiveness of world's petroleum source rocks. *U.S. Geological Survey Bulletin 1931*.

VINCENT E. & BERGER W. H. 1985. *Carbon dioxide and polar cooling in the Miocene: The Monterey Hypothesis* (The carbon cycle and atmospheric CO2: Natural variations Archean to present). American Geophysical Union, Washington, D.C.

WADE B. 2010. Philips XL30 Scanning Electron Microscope operating instructions.

WEILER R. & MILLS A. 1965. Surface properties and pore structure of marine sediments. *Deep Sea Research* **12**, 511-529.

ZONNEVELD K., VERSTEEGH G., KASTEN S., EGLINTON T., EMEIS K., HUGUET C., KOCH B., LANGE G., DE LEEUM J., MIDDELBURG J., MOLLENHAUER G., PRAHL F., RETHEMEYER J. & WAKEHAM S. 2009. Selective preservation of organic matter in marine environments – processes and impact on the fossil record. *Biogeosciences Discuss* **6**, 6371–6440.

FIGURE CAPTIONS

Figure 1: Map of the Californian Coast line adapted from Follmi et al (2005), showing location of Naples Beach (black box) and inclusion of the Santa Barbara Basin (dotted line).

Figure 2: Generalised stratigraphic column of the Monterey Formation Naples Beach Section, California (modified from DePaolo & Finger 1991) showing ages of the lithologic members (Isaacs, 2001)

Figure 3: Image showing naturally formed bitumen flowing up through the fractures. The image was taken at Naples Beach, east of the Dos Pueblos Creek. Courtesy of M.Kennedy.

Figure 4 a-c: Cross-plots of the lower member (a), middle member (b) and upper member (c) of the Monterey Formation. The x-axis is mineral surface area- CO_3 dilution and y-axis is % total organic carbon siliclastic. A one to one line is present in all plots. Identified loading rate for each lithology is calculated using a regression within that grouping with an overall relationship: R^2=0.53 lower member, R^2=0.85 middle member and R^2= 0.03 upper member. The middle member facies has a positive linear relationship.

Figure 5: % total organic carbon siliclastic cross-plot with mineral surface area- CO_3 dilution for the different lithologies present in the sampled area of the Monterey

Formation: laminated mudstone (diamond), nodular mudstone (square), phosphatic mudstone (triangle), carbonate cemented (open triangle), clayshale (circle), ash (open circle) and porcelanite (open diamond). A tightening of subsets occurs where there are positive linear relationships in the clay shale, laminated mudstone and carbonate cement lithologies. A one to one line is present in plot. The ethylene glycol monoethyl ether standards line, monolayer equivalent line was identified by measuring weight addition of ethylene glycol by a series of standards exposed to ethylene glycol monoethyl ether (Kennedy & Wagner 2011). The monolayer equivalent line is included to show a reference line only and does not imply that organic matter in natural samples occurs in a monolayer coating (Kennedy & Wagner 2011).

Figure 6: Cross-plot of mineral surface area- CO_3 dilution against % total organic carbon siliclastic for the different lithologies present in the sampled area of the Monterey Formation: laminated mudstone (diamond), carbonate cement (square), ash (circle) and porcelanite (triangle). The ash lithology is present to show a relationship of high mineral surface area but no total organic carbon. The porcelanite lithology is also plotted to show and compare a significant surface area with little preservation of carbon. The laminated mudstone and carbonate cement lithologies show a positive linear relationship. Identified loading rate for each lithology is calculated using a regression within that grouping with an overall relationship: R^2= 0.66 (laminated mudstone) and R^2=0.81 (carbonate cemented). A one to one line is present in the plot as well as a monolayer equivalent line. The ethylene glycol monoethyl ether standards line, monolayer equivalent line was identified by measuring weight addition of

ethylene glycol by a series of standards exposed to ethylene glycol monoethyl ether (Kennedy & Wagner, 2011). The monolayer equivalent line is included to show a reference line only and does not imply that organic matter in natural samples occurs in a monolayer coating (Kennedy & Wagner 2011).

Figure 7: Cross-plot of mineral surface area- CO_3 dilution against %total organic carbon siliclastic for the different lithologies present in the sampled area of the Monterey Formation: nodular mudstone (square), phosphatic mudstone (triangle), clayshale (circle), ash (diamond) and porcelanite (open circle). The ash lithology is present to show a relationship of high mineral surface area but no total organic carbon. The porcelanite lithology is also plotted to show and compare a significant surface area with little preservation of carbon. The nodular mudstone, phosphatic mudstone and clayshale have a positive linear relationship. Identified loading rate for each lithology is calculated using a regression within that grouping with an overall relationship: R^2= 0.66 (laminated mudstone) and R^2=0.81 (carbonate cemented). A one to one line is present in the plot as well as a monolayer equivalent line. The ethylene glycol monoethyl ether standards line, monolayer equivalent line was identified by measuring weight addition of ethylene glycol by a series of standards exposed to ethylene glycol monoethyl ether (Kennedy & Wagner 2011). The monolayer equivalent line is included to show a reference line only and does not imply that organic matter in natural samples occurs in a monolayer coating (Kennedy & Wagner 2011).

Figure 8: Cross-plot of the effect of organic matter removal on surface area of sediments in the Monterey Formation. Organic matter removed samples were treated

with hydrogen peroxide whereas the untreated samples were not. Removal of the organic matter tended to cause variable effects on the mineral surface area. Across the majority of the samples a tendency existed for the sediments to give higher surface area in the presence of organic matter. The cross plot also shows a one-one line (dashed).

Figure 9: The following figure shows: a) environmental scanning electron microscope image of a diatom on the surface using secondary electron detector at a scale of 50µm (magnification 2772 x). b) secondary electron image showing the edge of a diatom where the clay plates occur, which has an affiliation with carbon at a scale of 10 µm (magnification 13960 x). c) Carbon map of a diatom where no discrete areas of organic matter are visible at a scale of 20 µm. d) point analysis plot showing that the carbon is occurring, and that the high peak accounts for the carbon occurring around the edge of diatom, where the clay plates occurred.

Figure 10: Schematic figure illustrating a feedback system of carbon burial and seasonal climate. Showing that carbon burial increases as it gets warmer (wet, glacial period), until there is too much carbon buried. This then forces the climate to become colder driving the system back down again (seasonal, interglacial period).

Figure 11: A schematic figure showing mineral surface area vs total organi carbon in regards to divergence in the data set. A monolayer equivalent line is present as a comparison. There is a sequence of samples that fall off the line and this is indicative of

a series of processes involved in carbon loss (B). A number of samples (A) are above the line are attributed to carbon gain. Carbon loss can be attributed to thermogenic degradation or microbial respiration, carbon gain can be attributed to multilayer loading or particulate carbon.

Figure 12: The following figure shows an image of the Monterey Formation beach (a), a graph of total organic carbon vs depth taken and adapted from Mayer (1994) (b) showing that particulate organic matter only survives to a depth of 20cm below the seafloor, a cross-plot showing relationship between mineral surface area in m^2g^{-1} silicate fraction and %TOC siliclastic taken and adapted from Kennedy & Wagner (2011) (c). The Monterey Formation data from this paper has been added to the cross-plot allowing the formation of a comparison (c). The monolayer equivalent line was identified by measuring weight addition of ethylene glycol by a series of standards exposed to ethylene glycol monoethyl ether (Kennedy & Wagner 2011); it is included to show a reference line only and does not imply that organic matter in natural samples occurs in a monolayer coating (Kennedy & Wagner 2011). (c) An environmental scanning electron microscope image of a sample of the Monterey Formation also present where no particulate organic matter was observed on the surface (d).

Figure 13: A schematic figure showing four different models for surface loading A, B, C and D. Models A and B show carbon addition, where A is limited by surface area and is saturated by organic matter, and B has the same slope as the monolayer equivalent

line but has greater number of interlayer sites for loading. Models C and D show carbon loss where C has lost a proportionality of carbon through the oxidation of the external edges of the loading sites; however it is still proportional to mineral surface area. Model D is organic matter limited where the loading rate is smaller than the other models; leading to excess surface area.

TABLES

Table 1: Lithologies identified in the studied section of the Monterey Formation at Naples Beach

LITHOLOGY	DESCRIPTION
Laminated mudstone	a grey to black coloured mudstone characterised by the regular occurrence of light-coloured phosphatic laminae
Nodular mudstone	grey to dark coloured mudstone characterised by frequent phosphatic particles and nodules; where phosphatic laminae are less abundant
Phosphatic mudstone	grey coloured mudstone where granular phosphatic layers and isolated phosphatic nodules are frequent, phosphatic laminae are less abundant
Carbonate Cemented Claystone	Light coloured with no visible grain size
Ash	yellow to grey coloured in composition, very fine grain size, no phosphatic presence
Clay shale	grey to dark coloured shale characterised by fine grains and no laminae or phosphatic intervals present
Porcelanite	laminated fine grained clay stone, white to yellow in colour

APPENDICES

sample number	Determination of MSA								
	weight of initial container (g)	initial container + sample (g)	initial container + sample DRY (g)	sample mass (g)	final container + sample + EGME[1] (g)	mass EGME[1] (g)	mass EGME[1] (mg)	Surface area (m^2/g) H	MSA[2]-CO3 dilution
060105 /06									
2	17.0280	18.0397	18.0138	1.0116	18.0897	0.0759	75.9500	240.2531	269.7268
3	17.1767	18.1804	18.1578	1.0036	18.2192	0.0614	61.4000	195.7742	217.4021
5	17.1814	18.1860	18.1728	1.0510	18.2287	0.0558	55.8100	169.9339	217.7028
6	17.1759	18.1914	18.1774	1.0155	18.2373	0.0599	59.9000	188.7571	257.9172
10	17.2011	18.1561	18.1147	0.9550	18.1929	0.0782	78.1900	261.9952	310.3503
11	17.3488	18.4143	18.3712	1.0657	18.4469	0.0756	75.6500	227.1516	305.0631
12	17.1688	18.2662	18.2466	1.0974	18.3321	0.0855	85.4900	249.2988	292.8345
18 a	17.2527	18.3001	18.2591	1.0474	18.3915	0.1323	132.3100	404.2199	485.8614
18 b	17.6840	18.2066	18.1707	0.7804	18.2337	0.0630	63.0200	258.4111	316.1039
19	17.2982	18.3474	18.30714	1.0492	18.3757	0.0685	68.5500	209.0746	291.1422
20	17.5365	18.5778	18.5305	1.0412	18.6361	0.1056	105.6300	324.6299	358.8888
22	17.2169	18.2794	18.2362	1.0624	18.3432	0.1070	107.0000	322.2785	379.4061
23	17.1803	18.2448	18.2240	1.0644	18.2865	0.0625	62.4800	187.8383	257.9061
24	17.1416	18.1733	18.1432	1.0316	18.1917	0.0485	48.5200	150.5065	209.7562

25	17.1337	18.1915	18.1664	1.0577	18.2179	0.0515	51.5300	155.8939	300.879634
26	17.1334	18.1655	18.1432	1.0320	18.1949	0.0517	51.6900	160.2721	243.9493
28	17.2071	18.3055	18.2596	1.0984	18.3885	0.1289	128.9000	375.5400	377.9234
29	17.2188	18.2930	18.2778	1.0741	18.3283	0.0505	50.4800	150.3871	158.5549
30	17.2155	18.2805	18.2583	1.0650	18.3374	0.0791	79.1100	237.7115	301.1698
31	17.0612	18.0664	18.0367	1.0051	18.1263	0.0896	89.6200	285.3231	395.7911
32	17.2524	18.2552	18.2157	1.0026	18.3399	0.1242	124.1700	396.3037	396.3037
33	17.2781	18.3002	18.2750	1.0221	18.4200	0.1451	145.0500	454.1239	454.1239
34	17.2959	18.3774	18.3419	1.0814	18.4570	0.1151	115.0700	340.5036	348.2014
35	17.1291	18.2379	18.2158	1.1088	18.3687	0.1530	152.9500	441.4221	442.3689
36/1	17.5217	18.6095	18.6027	1.0877	18.6276	0.0249	24.8500	73.1074	173.5736
36/2	17.1667	18.2816	18.2727	1.1148	18.2986	0.0259	25.9500	74.4867	185.2600
37	17.2789	18.2993	18.2674	1.0203	18.3312	0.0639	63.8700	200.3126	224.9933
38	17.1367	18.2010	18.1669	1.0642	18.2257	0.0588	58.8200	176.8690	212.8970
40	17.2861	18.3745	18.3366	1.0884	18.4064	0.0698	69.8200	205.2765	224.4405
41	17.1553	18.1902	18.1668	1.0349	18.2405	0.0738	73.7700	228.1065	228.6959
42	17.0064	18.0953	18.0673	1.0887	18.1672	0.0999	99.9300	293.7160	294.1553
43	17.0448	18.0514	18.0243	1.0066	18.08856	0.0643	64.2500	204.2621	204.6625
45	17.2683	18.2977	18.2865	1.0293	18.3768	0.0902	90.2100	280.4465	281.0268
47	17.1296	18.2097	18.1816	1.0799	18.2622	0.0806	80.5900	238.8040	239.5754
48	17.3457	18.4177	18.3855	1.0719	18.4974	0.1119	111.9100	334.0831	336.1499
49	17.3274	18.4274	18.3991	1.0999	18.5028	0.1037	103.7200	301.7501	303.5125
50	17.4167	18.4464	18.4190	1.0297	18.5090	0.0900	90.0000	279.6999	279.6999
52	17.3128	18.4004	18.3829	1.0875	18.4488	0.0659	65.8800	193.8565	246.7694
53	17.1758	18.2584	18.2302	1.0824	18.2858	0.0556	55.6400	164.4907	174.4718
55	17.0429	18.1297	18.1006	1.0867	18.1811	0.0804	80.4300	236.8451	248.6368

56	17.2176	18.2886	18.2624	1.0710	18.3374	0.0749	74.9300	223.8815	230.6074
57	16.9521	18.0412	18.0169	1.0890	18.1076	0.0906	90.6300	266.3202	287.9412
58	17.2642	18.2767	18.2534	1.0125	18.3231	0.0697	69.7000	220.2951	255.3547
59	17.2500	18.3366	18.3062	1.0865	18.3886	0.0823	82.3300	242.4925	276.0942
60	17.2139	18.2897	18.27498	1.0758	18.3079	0.0330	32.9600	98.0442	178.7059
61	17.1353	18.1685	18.1377	1.0332	18.2426	0.1049	104.8600	324.7744	397.6815
62	17.0843	18.1434	18.1153	1.0591	18.2763	0.1611	161.0700	486.6600	507.9706
22406/02									
1	17.4297	18.4998	18.4644	1.0701	18.5202	0.0558	55.8300	166.9589	197.0522
2	17.2621	18.3448	18.3186	1.0827	18.3672	0.0487	48.6600	143.8149	144.2750
3	17.2479	18.2938	18.2545	1.0459	18.3184	0.0639	63.9200	195.5665	196.7228
5	17.1697	18.2435	18.2291	1.0738	18.2758	0.0467	46.6600	139.0507	174.1190
7	17.4395	18.5334	18.5199	1.0939	18.5798	0.0599	59.9100	175.2595	175.8164
11	17.1984	18.2678	18.2468	1.0692	18.3005	0.0537	53.7300	160.8021	169.5933
12	17.3869	18.4137	18.3809	1.0267	18.4792	0.0983	98.2800	306.3203	359.6318
13	17.2499	18.3079	18.2838	1.0581	18.3586	0.0749	74.8700	226.4381	362.0716
14	17.1292	18.1986	18.1623	1.0695	18.2248	0.0624	62.4400	186.8264	233.7186
15	17.1732	18.2609	18.2477	1.0876	18.3230	0.0753	75.2800	221.4912	292.9638
16	17.2643	18.2745	18.2561	1.0102	18.3353	0.0792	79.1800	250.8264	282.2309
17	17.1172	18.1661	18.1485	1.0490	18.2223	0.0738	73.7600	225.0174	273.3118
18	17.1375	18.2058	18.1743	1.0683	18.2362	0.0619	61.9400	185.5342	252.6588
20	17.3416	18.3960	18.3599	1.0544	18.4379	0.0780	77.9500	236.5728	317.6024
21	17.3133	18.3912	18.3738	1.0779	18.4590	0.0853	85.2800	253.1855	301.8746
22	17.2518	18.3058	18.2853	1.0539	18.3800	0.0947	94.7200	287.5995	365.0469
23	17.2811	18.3447	18.3330	1.0636	18.4050	0.0720	71.9800	216.5596	323.0498
24	17.3407	18.3810	18.3580	1.0402	18.4273	0.0693	69.3000	213.1816	325.5380

25	17.2331	18.3063	18.2865	1.0731	18.3349	0.0484	48.4500	144.4759	278.8232
26	17.2547	18.2855	18.2653	1.0308	18.3055	0.0402	40.2200	124.8644	233.5043
27	17.0699	18.0950	18.0739	1.0250	18.1427	0.0687	68.7400	214.6040	304.4215
30	17.0705	18.1115	18.0851	1.0410	18.1774	0.0923	92.3000	283.7176	332.6068
31	17.1382	18.1834	18.1640	1.0452	18.2759	0.1119	111.8900	342.5543	355.2720
32	17.0139	18.0917	18.0757	1.0778	18.1862	0.1104	110.4400	327.8976	330.4940
33	17.3077	18.3195	18.3040	1.0117	18.4071	0.1031	103.1055	326.1123	401.8234
34	17.3163	18.4213	18.4046	1.1051	18.4991	0.0945	94.5000	273.6503	379.2402
35	17.4910	18.4992	18.4795	1.0082	18.5768	0.0973	97.3000	308.8230	386.8960
36	17.2562	18.3074	18.2922	1.0511	18.3827	0.0906	90.5500	275.6731	437.4736
37	17.0778	18.0988	18.0825	1.0210	18.1897	0.1072	107.2100	336.0206	418.4035
38	17.0410	18.0314	18.0133	0.9904	18.1136	0.1003	100.2700	323.9676	415.6275
39	17.1777	18.2491	18.2258	1.0714	18.3276	0.1018	101.7900	304.0351	399.9800
40	17.3537	18.3736	18.3561	1.0199	18.4436	0.0875	87.5200	274.6035	319.4882
41	17.2837	18.3113	18.2939	1.0276	18.4004	0.1066	106.5700	331.8645	477.8905
42	17.2583	18.3337	18.3178	1.0754	18.4311	0.1133	113.3100	337.1804	405.2787
43	17.3621	18.3570	18.3433	0.9948	18.4297	0.0863	86.3500	277.7700	367.8508
44	17.3181	18.3800	18.3614	1.0619	18.4888	0.1274	127.3500	383.7595	386.0560
45	17.2717	18.2890	18.2759	1.0173	18.4079	0.1321	132.0800	415.4623	419.9202
46	17.5065	18.5346	18.5138	1.0281	18.6611	0.1473	147.3100	458.5012	465.1429
47	17.3162	18.3896	18.3710	1.0735	18.5276	0.1567	156.6800	467.0697	516.5854
48	17.3186	18.3155	18.2984	0.9969	18.4129	0.1145	114.4600	367.4054	438.1134
49	17.2525	18.2503	18.2303	0.9977	18.3509	0.1206	120.5800	386.7378	496.2151
50	17.2198	18.2712	18.2561	1.0514	18.3446	0.0885	88.5300	269.4375	329.0901
50 B	17.1716	18.2654	18.2517	1.0938	18.3349	0.0831	83.1200	243.1720	270.6810
50C	17.5518	18.5487	18.5360	0.9969	18.6075	0.0715	71.5200	229.5803	284.2833

51	17.1221	18.2046	18.1882	1.0825	18.2873	0.0990	99.0300	292.7446	433.9359
52a	17.2781	18.3246	18.30987	1.0465	18.4239	0.1140	114.0500	348.7368	350.9156
52b	17.3484	18.3542	18.3368	1.0055	18.4572	0.1205	120.4500	383.3145	385.7095
53	17.1948	18.1190	18.0808	0.9242	18.1917	0.1109	110.9000	383.9820	444.4079
64	17.2730	18.3019	18.2697	1.0289	18.4026	0.1328	132.8200	413.1059	445.9705
100	17.2422	18.2598	18.2072	1.0175	18.2769	0.0698	69.7700	219.4295	220.8152
102	17.1670	18.2194	18.1709	1.0524	18.2419	0.0710	71.0500	216.0395	217.6304
SA2-1									
1	17.1342	17.6646	17.6369	0.5304	17.7733	0.1364	136.4200	823.1088	826.5192
2	17.0571	17.5784	17.5554	0.5213	17.6861	0.1307	130.7200		
3	17.1180	17.6269	17.6032	0.5088	17.7322	0.1290	129.0000	811.3128	813.6923
4	17.2997	17.8137	17.7884	0.5140	17.9192	0.1308	130.7700		
5	17.1197	17.6493	17.6139	0.5294	17.7460	0.1321	132.0800		
6	17.3451	17.8635	17.8345	0.5185	17.9603	0.1258	125.8000		
7	17.1642	17.6761	17.6462	0.5119	17.7749	0.1287	128.6500		
8	17.1526	17.6749	17.6419	0.5223	17.7726	0.1308	130.7600		
9	17.1200	17.6378	17.6049	0.5178	17.7365	0.1316	131.5900		
10	17.3589	17.8817	17.8531	0.5228	17.9842	0.1311	131.1300		
STD	17.1584	17.6867	17.6582	0.5283	17.7921	0.1339	133.8800		
MANCOS									
1	17.2174	18.1339	18.1022	0.9164	18.1620	0.0598	59.7800	208.7427	212.2142
2	17.2530	18.1743	18.1414	0.9207	18.2017	0.0603	60.3300		
3	17.0513	17.9554	17.9239	0.9040	17.9838	0.0599	59.9500	212.2112	208.1324
4	16.9899	17.9038	17.8732	0.9139	17.9326	0.0594	59.4400		
5	17.1590	18.0645	18.0325	0.9055	18.0908	0.0584	58.3700		
6	17.2192	18.1320	18.1001	0.9128	18.1599	0.0598	59.7600		

7	17.2878	18.1955	18.1615	0.9076	18.2219	0.0604	60.4100		
8	17.0492	17.9644	17.9344	0.9151	17.9946	0.0602	60.2200		
9	17.0162	17.9218	17.8854	0.9055	17.9450	0.0596	59.6500		
10	17.1178	18.0294	17.9984	0.9116	18.0587	0.0603	60.3000		
OM² removed 060105/06									
2	17.3625	18.3830	18.3511	1.0204	18.4118	0.0608	60.7700	190.5706	209.3518
3	17.2431	18.3314	18.2878	1.0881	18.3688	0.0810	81.0000	238.2079	255.2580
4	17.0591	18.1206	18.0963	1.0615	18.1348	0.0385	38.4900	116.0331	174.4134
6	17.2943	18.3351	18.3075	1.0406	18.3546	0.0472	47.1900	145.1128	198.6562
7	17.1326	18.1844	18.1597	1.0518	18.2083	0.0486	48.5900	147.8367	180.6204
8	17.3154	18.3402	18.2966	1.0246	18.3533	0.0567	56.6700	176.9987	204.7746
9	17.0231	18.0236	17.9817	1.0004	18.0479	0.0662	66.2100	211.7820	250.3704
10	17.0835	18.1232	18.0850	1.0397	18.1520	0.0670	67.0100	206.2491	233.6227
12	17.3009	18.3570	18.3173	1.0560	18.3854	0.0681	68.1400	206.4760	246.5406
13	17.2540	18.2652	18.2329	1.0112	18.2897	0.0567	56.7300	179.5200	221.2372
15	17.3285	18.3982	18.3872	1.0697	18.4136	0.0263	26.3300	78.7656	253.6169
16	17.3328	18.4075	18.3747	1.0746	18.4502	0.0755	75.4900	224.7928	286.0919
19	17.3141	18.3554	18.3229	1.0412	18.3580	0.0351	35.0900	107.8417	152.4651
20	17.3344	18.3791	18.3428	1.0446	18.3956	0.0528	52.7800	161.6887	164.6940
22	17.2089	18.2693	18.2388	1.0603	18.2916	0.0528	52.7900	159.3194	175.4204
25	17.1805	18.2116	18.1947	1.0310	18.2210	0.0263	26.3100	81.6589	160.3000
26	17.2795	18.3108	18.2910	1.0310	18.3217	0.0307	30.7200	95.3464	162.9752
27	17.3730	18.4227	18.3918	1.0498	18.4384	0.0466	46.5900	142.0197	155.6333
29	17.3131	18.3685	18.3579	1.0552	18.3805	0.0226	22.5800	68.4768	73.6502
30	17.0873	18.1292	18.1183	1.0419	18.1373	0.0190	18.9800	58.2915	72.4517

sample number	Determination of TOC[3]				
	(g)	(ml)	TOC[3]	*% Carbonate*	TOC[3] Carbonate
060105 /06					
2	1.01	20.80	7.23	10.93	8.12
3	0.99	18.60	4.37	9.95	4.86
5	1.00	41.40	1.56	21.94	2.00
6	1.02	51.40	3.94	26.81	5.38
10	1.03	30.20	6.14	15.58	7.27
11	1.01	48.60	3.67	25.54	4.93
12	1.02	28.40	3.91	14.87	4.59
18 a	1.00	31.60	18.38	16.80	22.09
18 b	1.03	35.40	4.13	18.25	5.05
19	1.01	53.60	11.25	28.19	15.67
20	1.00	18.00	13.13	9.55	14.52
22	1.04	29.40	14.46	15.06	17.02
23	1.03	52.70	6.13	27.17	8.42
24	1.02	54.40	1.97	28.25	2.75
25	0.29	26.50	2.65	48.19	5.12
26	1.09	70.40	4.40	34.30	6.70
28	1.01	1.20	16.92	0.63	17.03
29	1.08	10.50	4.96	5.15	5.23

30	1.01	40.10	11.11	21.07	14.08
31	1.01	52.80	13.08	27.91	18.15
32	1.01	0.00	19.30	0.00	19.30
33	1.01	0.00	26.06	0.00	26.06
34	1.03	4.30	16.93	2.21	17.32
35	0.99	0.40	24.48	0.21	24.53
36/1	0.63	68.60	1.98	57.88	4.70
36/2	0.54	60.60	2.68	59.79	6.66
37	1.00	20.60	5.36	10.97	6.02
38	1.01	32.20	4.81	16.92	5.79
40	1.04	16.70	4.75	8.54	5.20
41	1.03	0.50	0.90	0.26	0.90
42	1.07	0.30	1.99	0.15	2.00
43	1.09	0.40	3.43	0.20	3.43
45	1.03	0.40	3.23	0.21	3.24
47	0.99	0.60	8.96	0.32	8.99
48	1.04	1.20	4.70	0.61	4.73
49	1.01	1.10	2.13	0.58	2.14
50	1.04	0.00	3.09	0.00	3.09
52	1.01	40.80	4.09	21.44	5.21
53	0.70	7.50	3.49	5.72	3.70
55	1.01	9.00	7.50	4.74	7.87
56	0.91	5.00	6.75	2.92	6.95
57	1.06	15.00	2.26	7.51	2.45
58	0.99	25.60	7.23	13.73	8.38
59	1.07	24.50	9.01	12.17	10.26

60	0.51	43.40	2.56	45.14	4.67
61	1.10	37.90	16.68	18.33	20.42
62	1.01	8.00	24.72	4.20	25.80
22406/02					
1	1.09	31.40	1.97	15.27	2.33
2	1.00	0.60	0.56	0.32	0.56
3	1.00	1.10	0.11	0.59	0.11
5	1.02	38.60	0.01	20.14	0.01
7	0.84	0.50	0.41	0.32	0.41
11	1.01	9.80	1.07	5.18	1.12
12	1.01	28.10	12.22	14.82	14.34
13	0.47	32.90	8.38	37.46	13.40
14	1.01	38.20	9.27	20.06	11.60
15	1.02	46.60	9.47	24.40	12.53
16	1.00	21.00	11.01	11.13	12.39
17	1.05	34.80	10.05	17.67	12.21
18	1.03	51.40	6.10	26.57	8.30
20	1.01	48.30	9.76	25.51	13.10
21	1.00	30.40	9.89	16.13	11.80
22	1.01	40.30	11.68	21.22	14.83
23	1.01	62.40	5.78	32.96	8.62
24	1.00	65.00	7.48	34.51	11.42
25	0.49	44.00	4.23	48.18	8.16
26	0.46	40.40	2.58	46.53	4.83
27	1.10	61.00	10.29	29.50	14.59
30	1.03	28.40	11.95	14.70	14.01

31	1.07	7.20	14.69	3.58	15.23
32	1.08	1.60	14.12	0.79	14.23
33	1.08	38.10	9.39	18.84	11.57
34	1.08	56.40	12.42	27.84	17.21
35	1.08	40.90	13.20	20.18	16.54
36	1.08	75.40	8.93	36.99	14.17
37	1.06	39.40	13.13	19.69	16.34
38	1.02	42.20	15.71	22.05	20.15
39	1.04	46.70	13.09	23.99	17.23
40	0.52	13.80	15.65	14.05	18.21
41	1.07	61.30	7.64	30.56	11.00
42	1.04	32.70	16.52	16.80	19.85
43	1.05	48.40	13.76	24.49	18.22
44	1.07	1.20	16.15	0.59	16.24
45	1.00	2.00	15.58	1.06	15.75
46	1.04	2.80	21.42	1.43	21.73
47	1.01	18.20	22.52	9.59	24.91
48	1.03	31.40	20.56	16.14	24.51
49	1.07	44.30	16.71	22.06	21.44
50	1.07	36.60	10.79	18.13	13.17
50 B	1.10	21.00	12.51	10.16	13.92
50C	1.00	36.20	6.41	19.24	7.94
51	1.05	64.00	6.66	32.54	9.88
52a	1.03	1.20	17.40	0.62	17.51
52b	1.03	1.20	19.02	0.62	19.14
53	1.05	26.80	17.70	13.60	20.48

64	**1.07**	**14.80**	**20.17**	**7.37**	**21.77**
100	**0.51**	**0.60**	**0.30**	**0.63**	**0.30**
102	**0.58**	**0.80**	**0.17**	**0.73**	**0.17**
SA2-1					
1	**0.32**	**0.25**	**0.02**	**0.41**	**0.02**
3	**0.18**	**0.10**	**0.02**	**0.29**	**0.02**
MANCOS					
1	**0.20**	**0.60**	**2.61**	**1.64**	**2.66**
3	**0.20**	**0.62**	**2.238**	**1.69**	**2.28**

[1] Ethylene Glycol Monoethyl Ether (EGME)

[2] Mineral Surface Area (MSA)

[3] Total Organic Carbon (TOC)

FIGURES

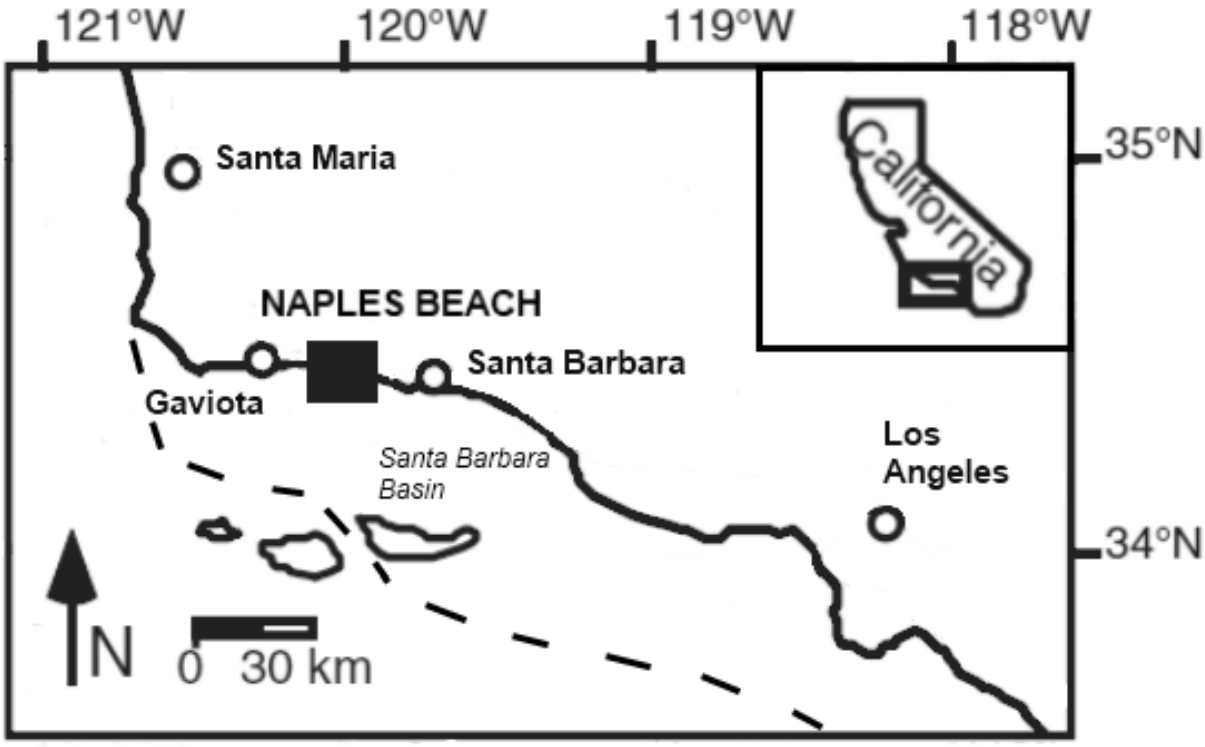

Figure 1

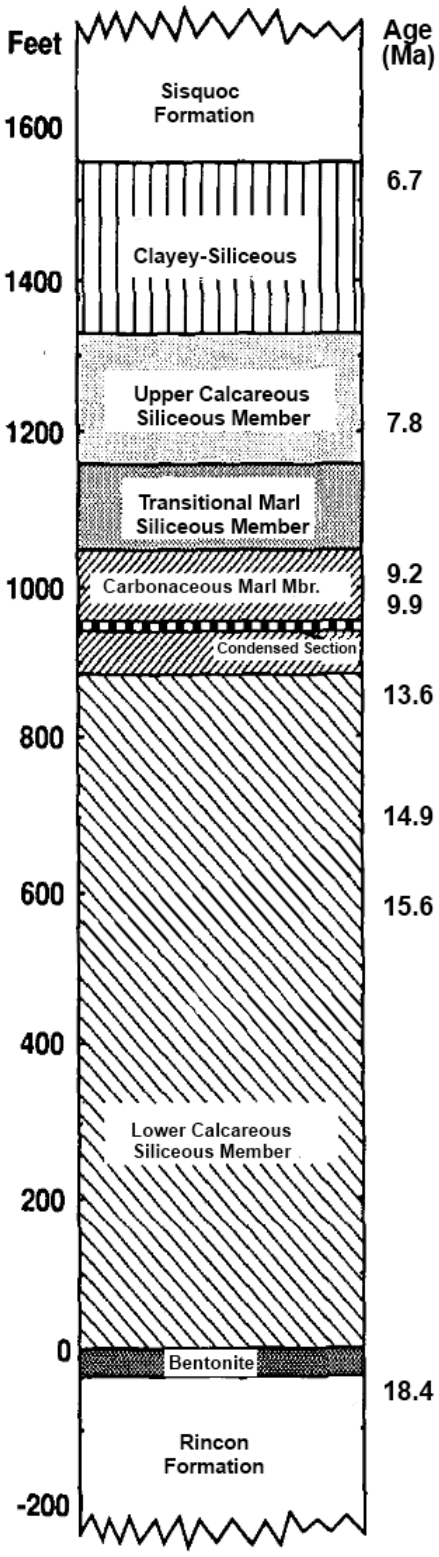
Feet
Age (Ma)
Sisquoc Formation
1600
6.7
Clayey-Siliceous
1400
Upper Calcareous Siliceous Member
7.8
1200
Transitional Marl Siliceous Member
Carbonaceous Marl Mbr.
9.2
9.9
1000
Condensed Section
13.6
800
14.9
600
15.6
400
Lower Calcareous Siliceous Member
200
0
Bentonite
18.4
Rincon Formation
-200

Figure 2

Figure 3

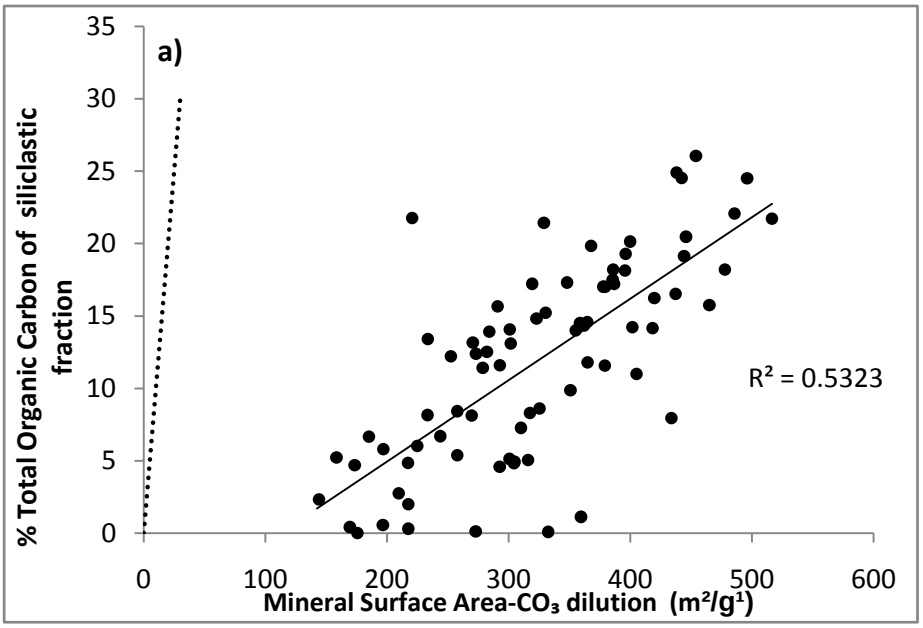
a)
% Total Organic Carbon of siliclastic fraction
Mineral Surface Area-CO₃ dilution (m²/g¹)
R² = 0.5323
0
5
10
15
20
25
30
35
0
100
200
300
400
500
600

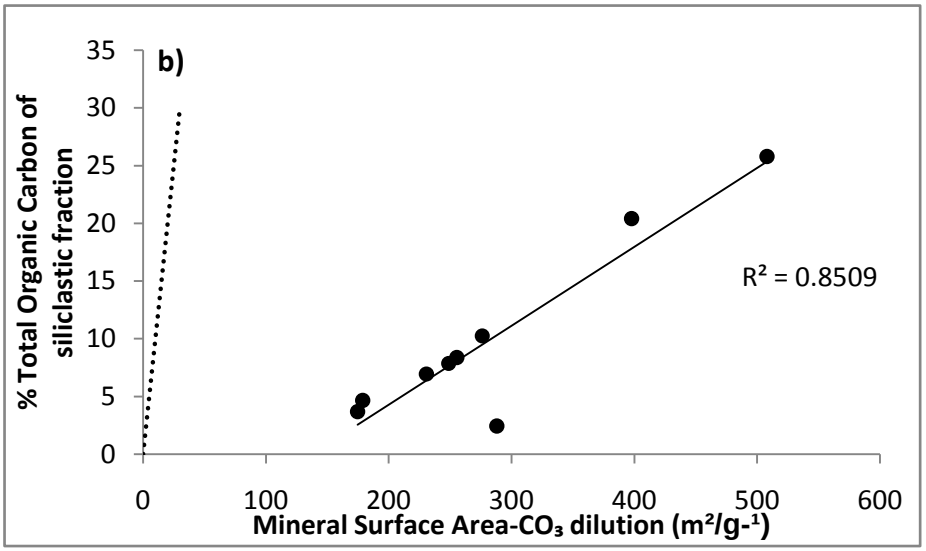
b)
% Total Organic Carbon of siliclastic fraction
Mineral Surface Area-CO₃ dilution (m²/g-¹)
R² = 0.8509
0
5
10
15
20
25
30
35
0
100
200
300
400
500
600

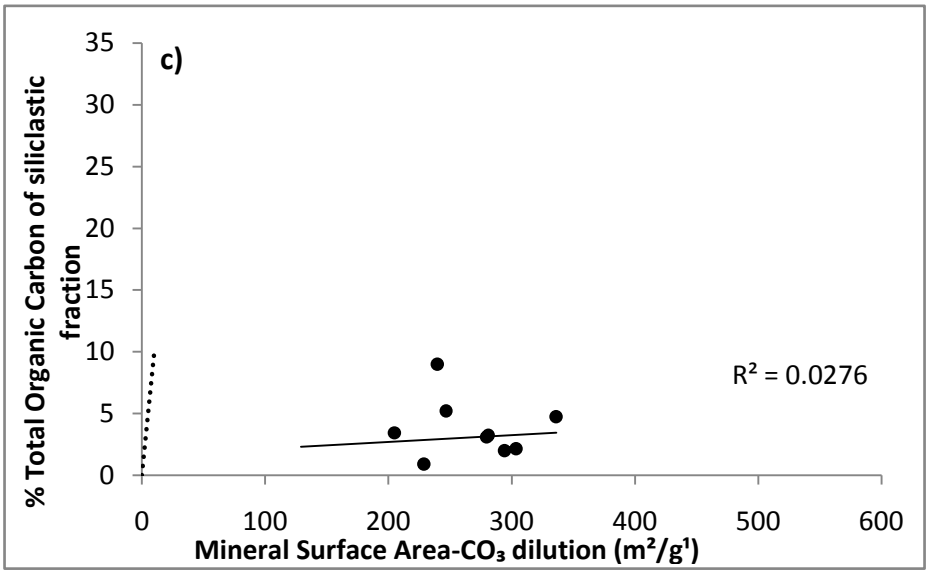
c)
% Total Organic Carbon of siliclastic fraction
Mineral Surface Area-CO₃ dilution (m²/g¹)
R² = 0.0276
0
5
10
15
20
25
30
35
0
100
200
300
400
500
600

Figure 4

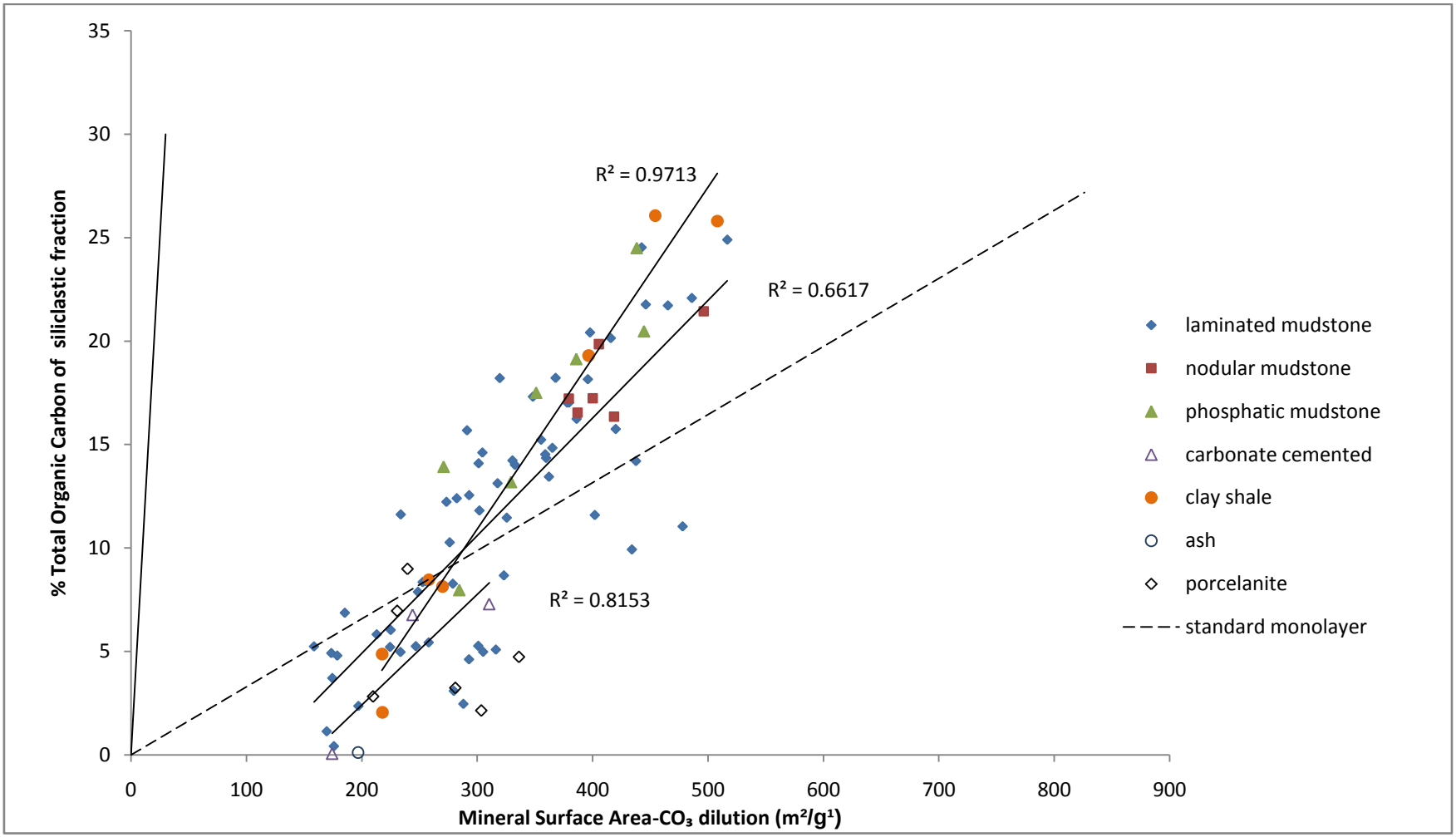
% Total Organic Carbon of siliclastic fraction
Mineral Surface Area-CO₃ dilution (m²/g¹)
R² = 0.9713
R² = 0.6617
R² = 0.8153
laminated mudstone
nodular mudstone
phosphatic mudstone
carbonate cemented
clay shale
ash
porcelanite
standard monolayer
0
5
10
15
20
25
30
35
0
100
200
300
400
500
600
700
800
900

Figure 5

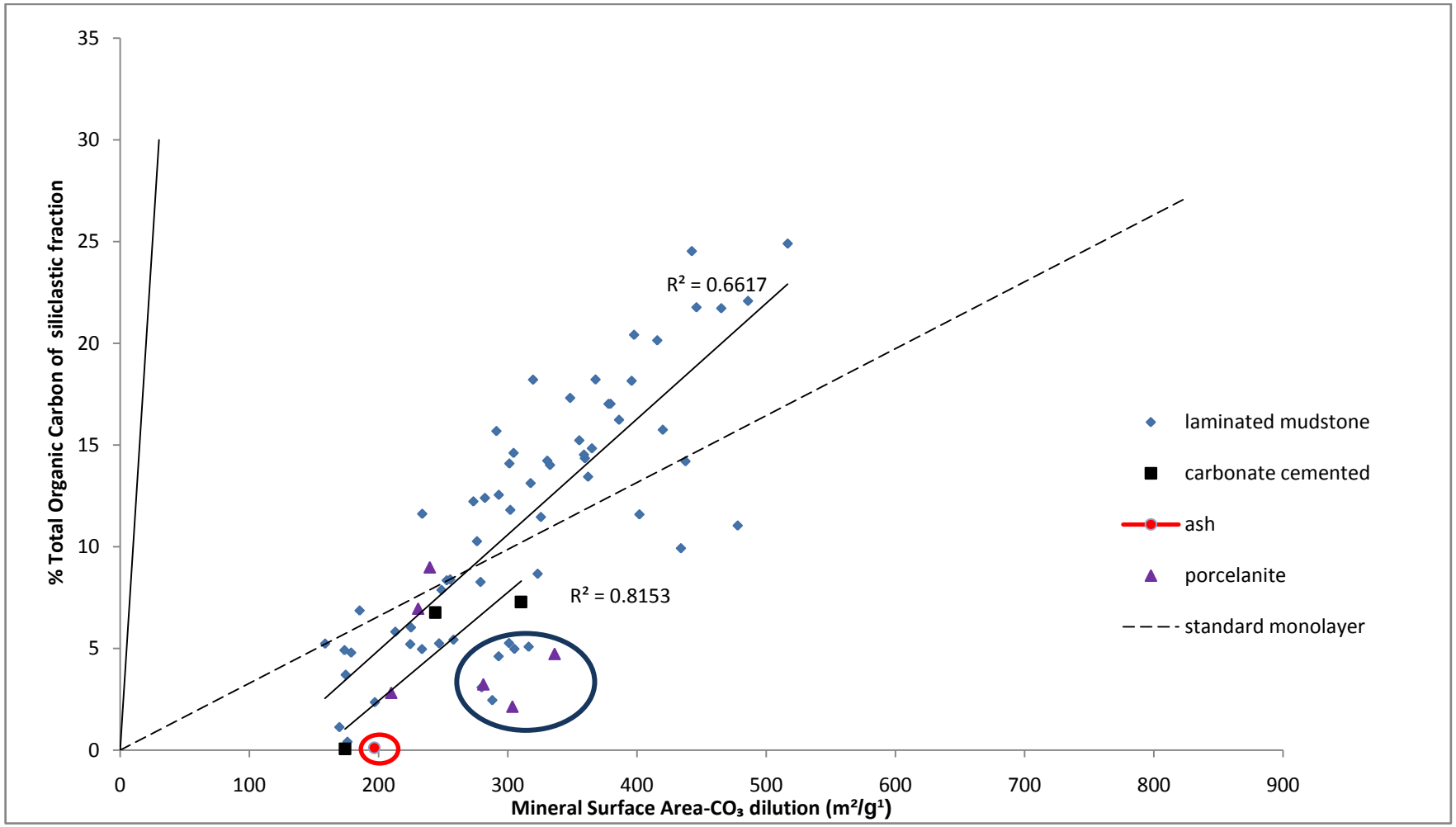
% Total Organic Carbon of siliclastic fraction
Mineral Surface Area-CO₃ dilution (m²/g¹)
R² = 0.6617
R² = 0.8153
laminated mudstone
carbonate cemented
ash
porcelanite
standard monolayer
0
5
10
15
20
25
30
35
0
100
200
300
400
500
600
700
800
900

Figure 6

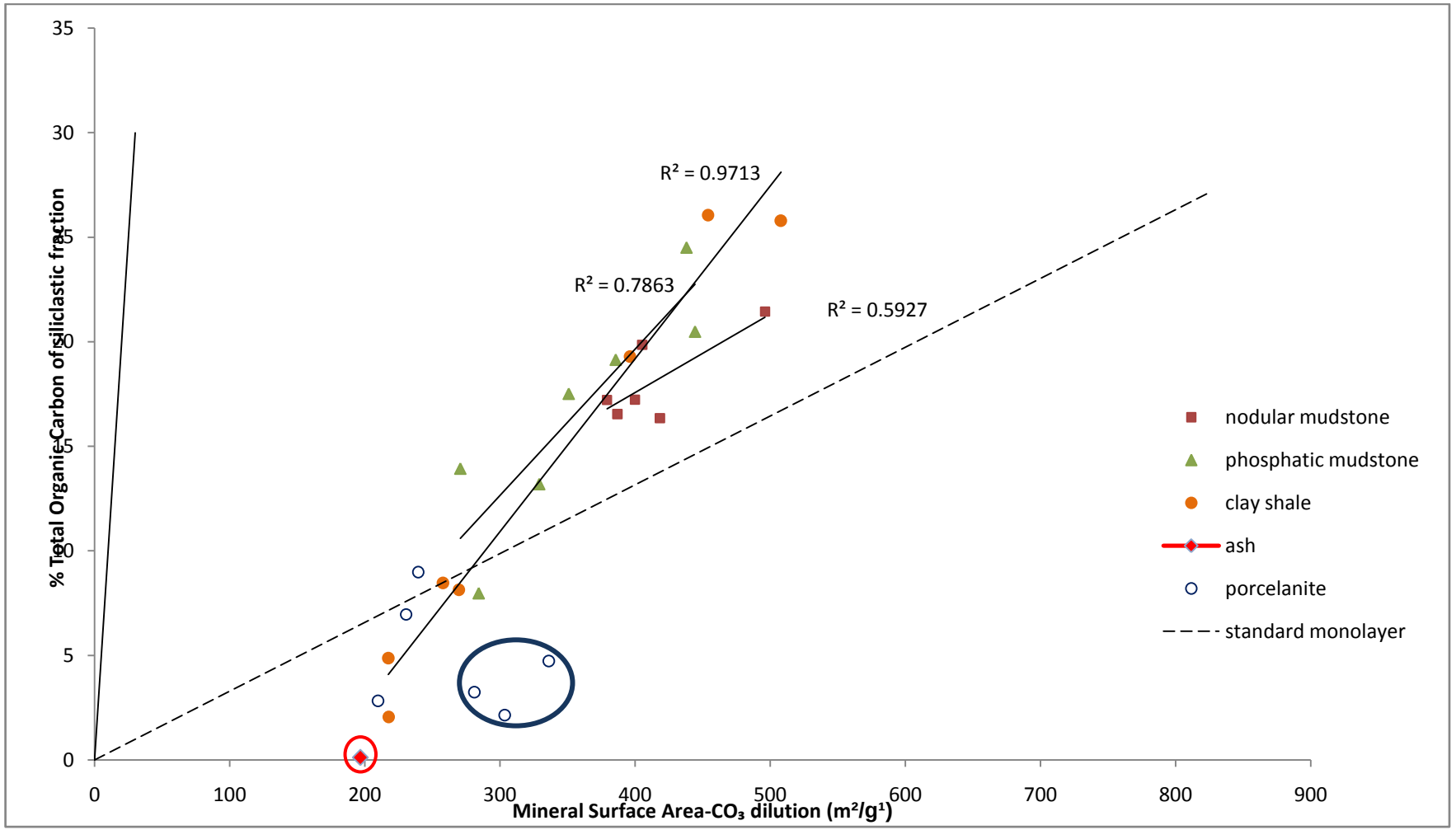
35
30
25
20
15
10
5
0
% Total Organic Carbon of siliclastic fraction
0
100
200
300
400
500
600
700
800
900
Mineral Surface Area-CO₃ dilution (m²/g¹)
R² = 0.9713
R² = 0.7863
R² = 0.5927
nodular mudstone
phosphatic mudstone
clay shale
ash
porcelanite
standard monolayer

Figure 7

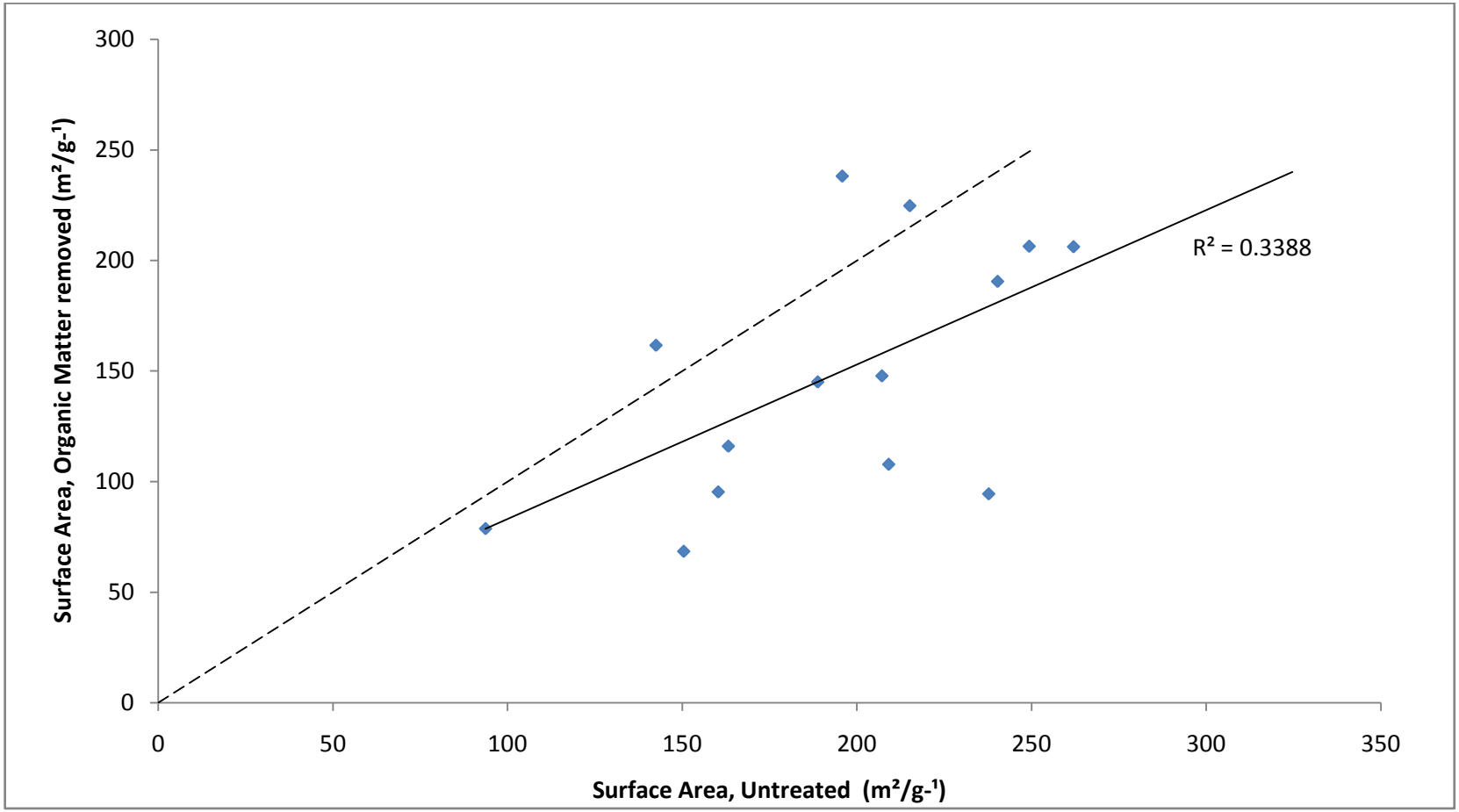
300
250
200
150
100
50
0
0
50
100
150
200
250
300
350
Surface Area, Organic Matter removed (m²/g-¹)
Surface Area, Untreated (m²/g-¹)
R² = 0.3388

Figure 8

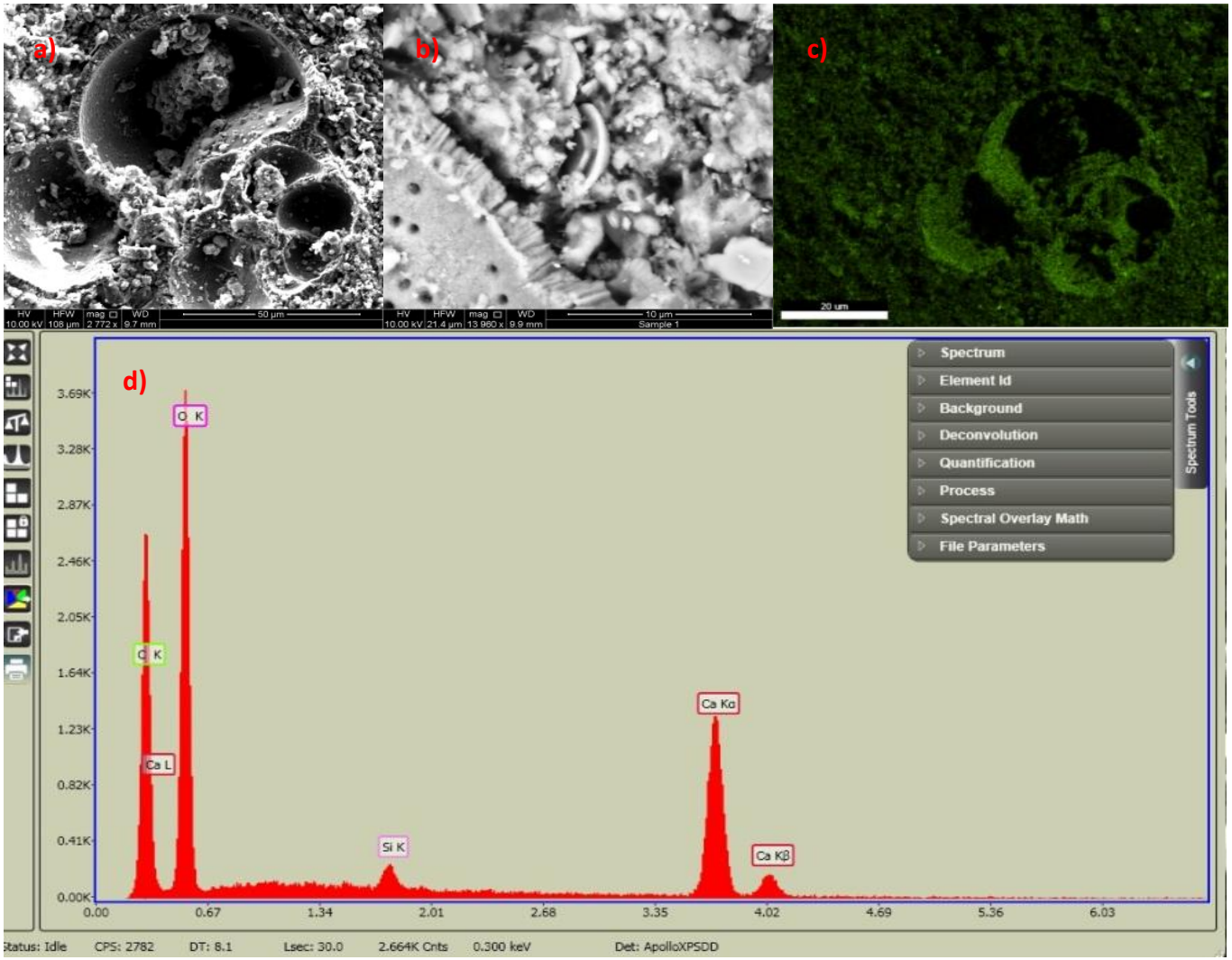
a)
b)
c)
d)
Spectrum
Element Id
Background
Deconvolution
Quantification
Process
Spectral Overlay Math
File Parameters
Spectrum Tools
O K
C K
Ca L
Si K
Ca Kα
Ca Kβ
3.69K
3.28K
2.87K
2.46K
2.05K
1.64K
1.23K
0.82K
0.41K
0.00K
0.00
0.67
1.34
2.01
2.68
3.35
4.02
4.69
5.36
6.03
Status: Idle
CPS: 2782
DT: 8.1
Lsec: 30.0
2.664K Cnts
0.300 keV
Det: ApolloXPSDD

Figure 9

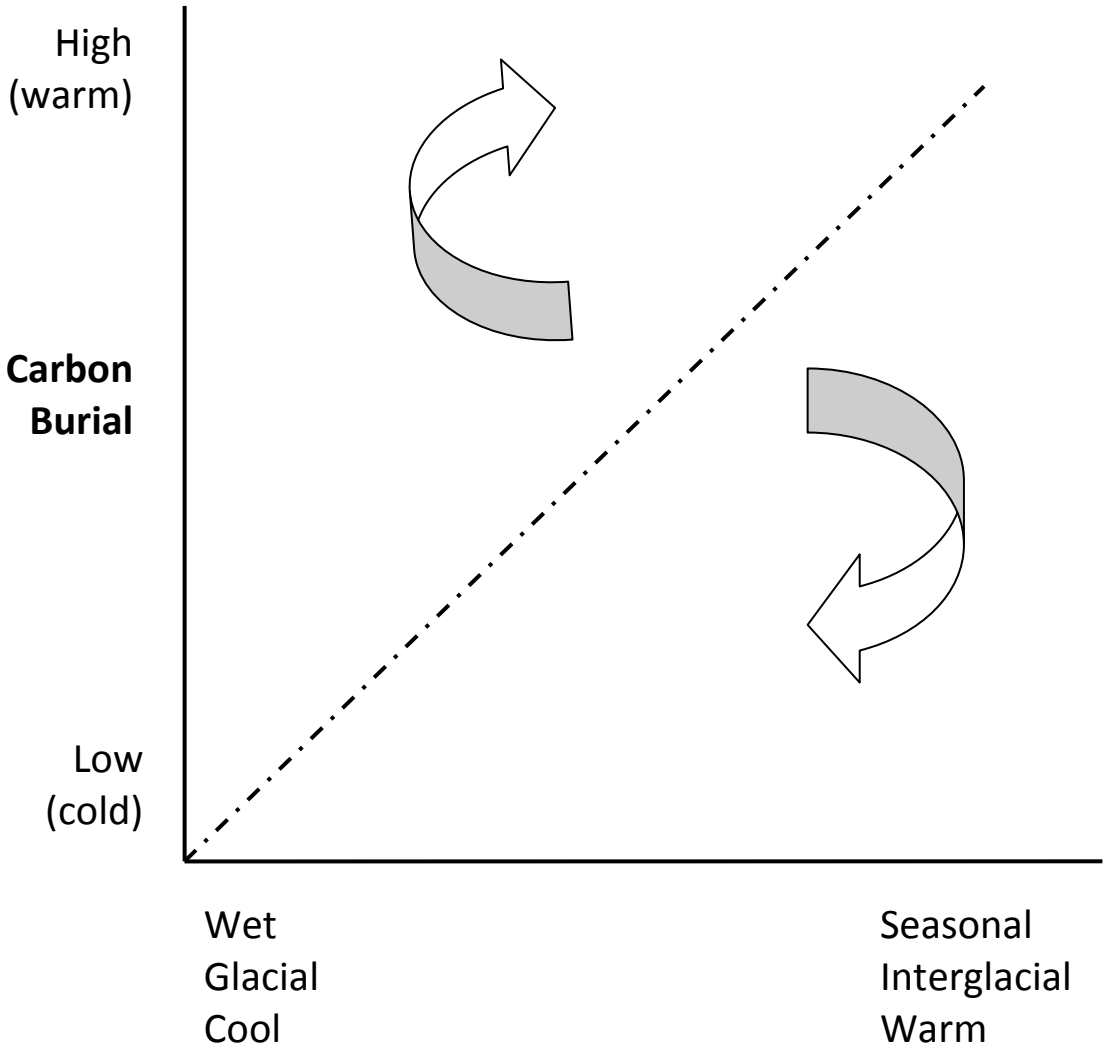
High
(warm)
Carbon
Burial
Low
(cold)
Wet
Glacial
Cool
Seasonal
Interglacial
Warm

Figure 10

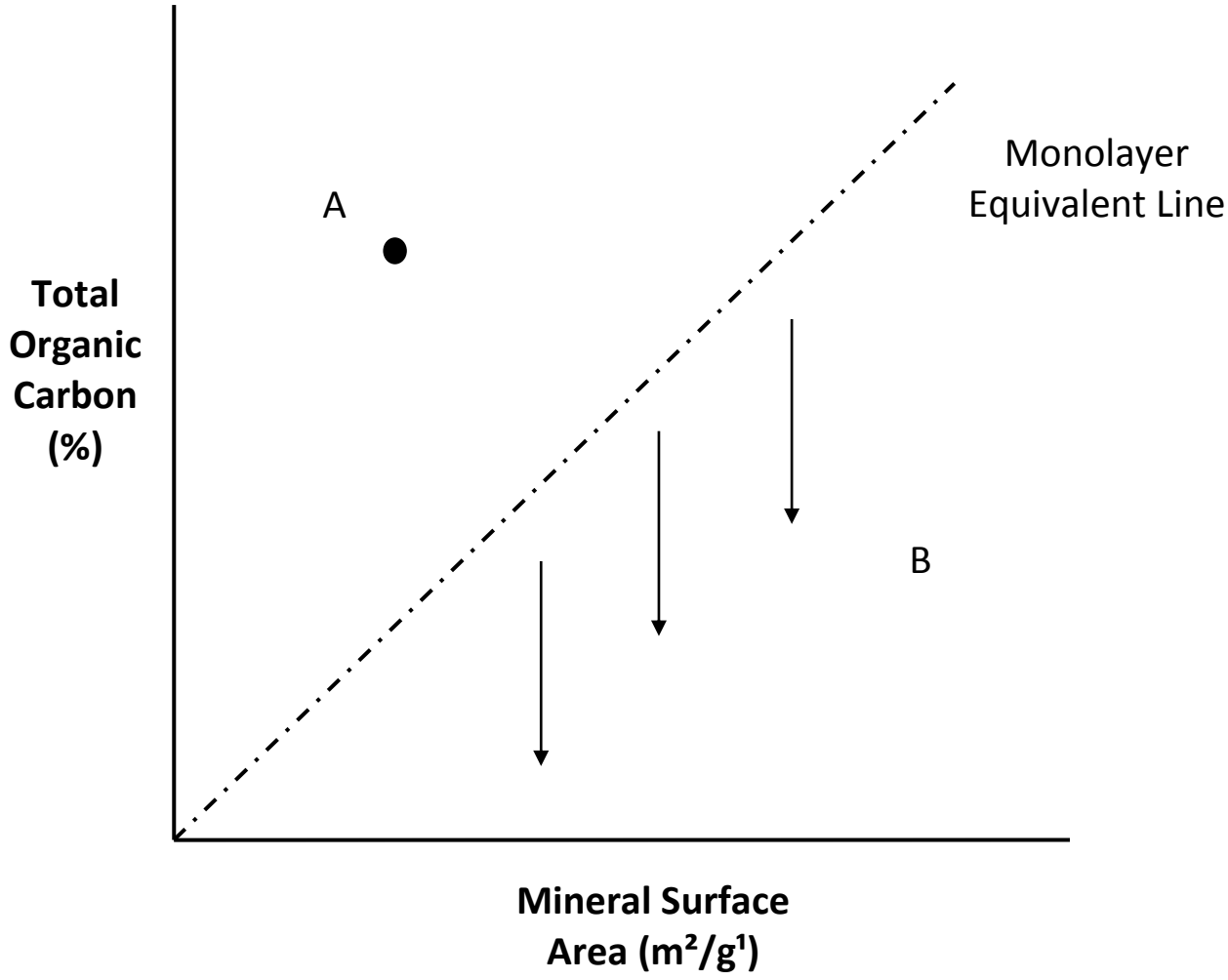
Monolayer
Equivalent Line
A
B
Total
Organic
Carbon
(%)
Mineral Surface
Area (m²/g¹)

Figure 11

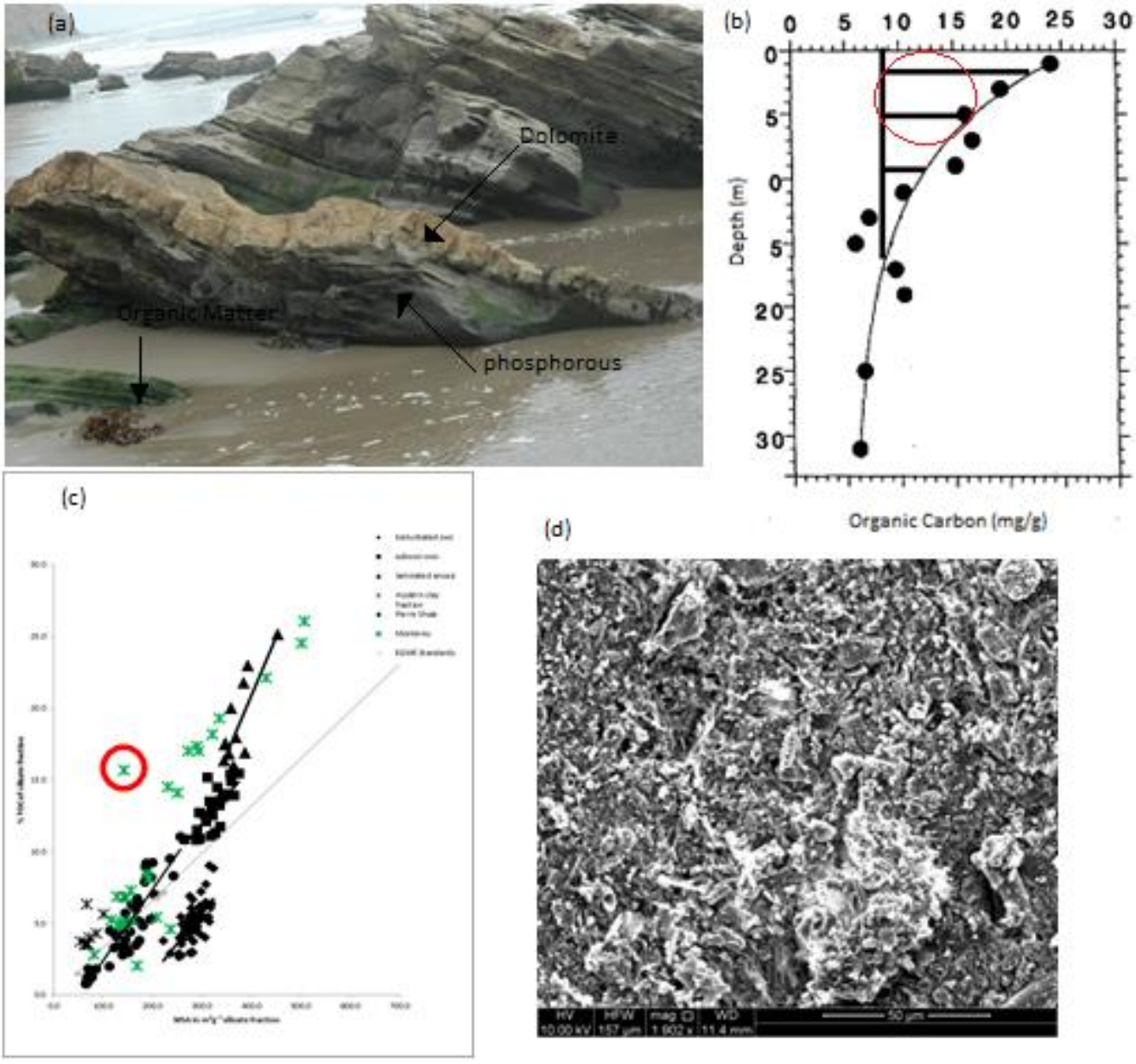
(a)
Dolomite
Organic Matter
phosphorous
(b)
0 5 10 15 20 25 30
Depth (m)
Organic Carbon (mg/g)
(c)
(d)

Figure 12

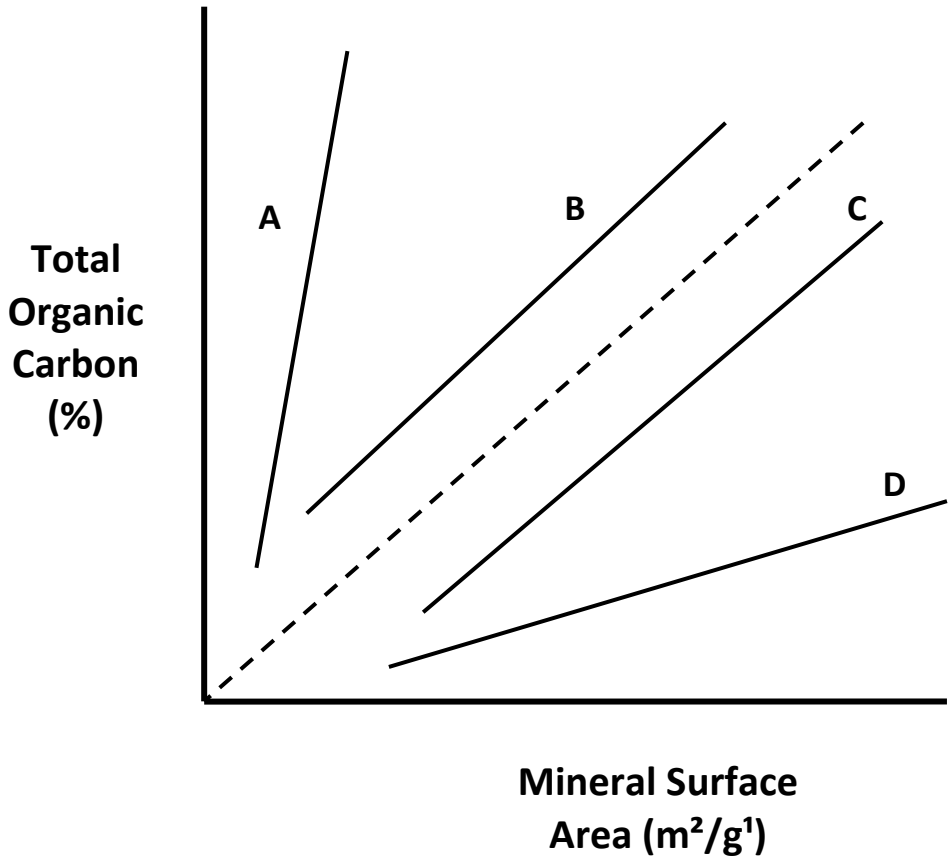

Figure 13